Neuroimaging in Dementia

Adam M. Staffaroni, PhD[1], **Fanny M. Elahi, MD, PhD**[1], **Dana McDermott, DO**[1], **Kacey Marton, MS**[1], **Elissaios Karageorgiou, MD, PhD**[1,2], **Simone Sacco, MD**[1,3], **Matteo Paoletti, MD**[1,3], **Eduardo Caverzasi, MD**[1,4], **Christopher P. Hess, MD, PhD**[5], **Howard J. Rosen, MD**[1], and **Michael D. Geschwind, MD, PhD**[1]

[1]Department of Neurology, Memory and Aging Center, University of California, San Francisco (UCSF), San Francisco, California

[2]Neurological Institute of Athens, Athens, Greece

[3]Institute of Radiology, Department of Clinical Surgical Diagnostic and Pediatric Sciences, University of Pavia, Pavia, Italy

[4]Department of Brain and Behavioral Sciences, University of Pavia, Pavia, Italy

[5]Division of Neuroradiology, Department of Radiology, University of California, San Francisco (UCSF), California

Abstract

Although the diagnosis of dementia still is primarily based on clinical criteria, neuroimaging is playing an increasingly important role. This is in large part due to advances in techniques that can assist with discriminating between different syndromes. Magnetic resonance imaging remains at the core of differential diagnosis, with specific patterns of cortical and subcortical changes having diagnostic significance. Recent developments in molecular PET imaging techniques have opened the door for not only antemortem but early, even preclinical, diagnosis of underlying pathology. This is vital, as treatment trials are underway for pharmacological agents with specific molecular targets, and numerous failed trials suggest that earlier treatment is needed. This article provides an overview of classic neuroimaging findings as well as new and cutting-edge research techniques that assist with clinical diagnosis of a range of dementia syndromes, with an emphasis on studies using pathologically proven cases.

The diagnosis of dementia is becoming increasingly reliant on a broad range of neuroimaging techniques, and this is reflected in several updated diagnostic criteria.[1,2] Neuroimaging enhances the accuracy of diagnoses for distinct dementia subtypes. The recent failures of treatment trials for Alzheimer's disease (AD)[3] indicate that earlier

Address for correspondence: Michael D. Geschwind, MD, PhD, Department of Neurology, Memory and Aging Center, University of California San Francisco (UCSF), Box 1207, San Francisco, CA 94143-1207 (Michael.Geschwind@ucsf.edu).

intervention, and therefore earlier diagnosis, may be critical to treatment success. Early diagnosis can be facilitated by neuroimaging techniques that can detect the earliest pathological and metabolic alterations that occur in neurodegenerative disease.

In this review, we discuss clinically relevant neuroimaging findings in a wide range of dementia syndromes, as well as cutting-edge techniques that are gaining traction in research. As we move toward the age of treatments designed for specific molecular targets (e.g., tau and amyloid), there is a growing need to move beyond simply classifying syndromes based entirely on clinical phenotypes to predicting underlying pathologies with greater precision using imaging, genetic, cerebrospinal fluid (CSF), and other objective markers of disease. In this review, we try to distinguish between imaging findings in pathologically proven versus clinically based diagnoses, placing particular emphasis on neuroimaging in pathologically confirmed cases as well as longitudinal neuroimaging studies. Dementia and related syndromes discussed in this review include AD, the frontotemporal dementia (FTD) spectrum, primary progressive aphasias (PPA), vascular dementia (VaD), Lewy body disease (LBD) and Parkinson's disease dementia (PDD), rapidly progressing dementias (RPD), normal pressure hydrocephalus (NPH), and cerebellar disorders. Other dementing conditions, including neurodegeneration with brain iron accumulation (NBIA) and chronic traumatic encephalopathy (CTE), are not covered here to allow for a greater depth of coverage of the more common and established causes of dementia. We conclude with a review of neuroimaging biomarkers of neurodegenerative diseases that are being developed in research, with a focus on structural and functional connectivity.

Alzheimer's Disease

Introduction

AD is a pathologic entity characterized by the aberrant aggregation of amyloid-β and tau proteins, which form neuritic plaques and neurofibrillary tangles (NFTs), respectively. These changes lead to neuronal dysfunction and death, with subsequent atrophy of selectively vulnerable brain networks and emergent clinical features, including cognitive impairment.[4] Depending on the brain regions and networks that are affected, AD can present with a multitude of clinical syndromes, including, but not limited to, the classic amnestic syndrome, posterior cortical atrophy (PCA), a frontal/dysexecutive syndrome, and the logopenic variant of primary progressive aphasia (discussed in the Primary Progressive Aphasia section). Substantial research efforts aimed at studying biomarkers of AD, including the large-scale Alzheimer's Disease Neuroimaging Initiative (ADNI) and the Imaging Dementia-Evidence for Amyloid Scanning (IDEAS) studies, have shown that neuroimaging biomarkers improve clinical diagnosis in AD. In fact, current AD diagnostic criteria incorporate neuroimaging as a biomarker because it increases the degree of diagnostic certainty that the clinical presentation reflects underlying AD pathology (i.e., probable versus possible AD).[2] Despite established criteria, however, AD remains a diagnostic and therapeutic challenge for several reasons. First, the clinical expression of AD is variable in its phenotypic (i.e., syndromic) and endophenotypic (e.g., network vulnerability or genetic) features.[5] Furthermore, the presence of AD pathology does not mean that cognitive deficits are detected, as about one-third of cognitively nonimpaired

people at around age 75, and half of those around age 85, have in vivo markers [amyloid positron emission tomography (PET) scan] of underlying AD pathology.[6] Additionally, AD pathology often co-exists with other pathologies, such as synucleinopathies and vascular disease, that contribute to cognitive deficits, raising uncertainty about direct causality between specific underlying pathology and predominant clinical syndrome.[7]

MRI

Although the earliest site of AD pathology is often phosphotau accumulation in brainstem nuclei,[8,9] the earliest atrophy on magnetic resonance imaging (MRI) is detected in the cerebrum.[10] In the classic amnestic AD syndrome, early atrophy can be appreciated in the hippocampi and precuneus (Fig. 1).[10] Interestingly, however, hippocampal atrophy is best linked to *APOE ε4* polymorphism and the amnestic pattern of late-onset Alzheimer's disease (LOAD), but may not be a primary feature of early-onset (EOAD) presentations, which have more early posterior cortical involvement.[11–13] Many LOAD atrophy patients also often have prominent posterior involvement,[14] irrespective of the syndromic presentation; this pattern often can assist the clinician in discriminating AD from other pathologies that can manifest with similar clinical syndromes. For example, corticobasal syndrome (CBS) is an FTD-spectrum disease that may be associated with AD or frontotemporal lobar degeneration (FTLD) pathology. Patients with CBS due to underlying AD pathology have parietal-predominant atrophy, in contrast to the frontal-predominant atrophy of CBS due to FTLD pathology.[15] Thus, identifying posterior-predominant atrophy (i.e., precuneus and posterior cingulate) on imaging is suggestive of underlying AD pathology, as it generally is a feature across AD syndromes (Fig. 1). Atrophy in AD is not always symmetric, such as in logopenic variant primary progressive aphasia (lvPPA) patients, in whom AD is the underlying pathology, and atrophy is first observed in the left temporoparietal junction.[16]

Identifying the above anatomical features often is aided by viewing structural (T1) brain images in different planes (Fig. 1). FDA- and CE-approved automated algorithms are now available in clinical practice for establishing areas of atrophy in a single subject compared with normal populations, as well as for evaluating progression of atrophy.[17] It remains to be seen how these programs will add to diagnostic accuracy in terms of their sensitivity and specificity, relationship to clinical outcomes and to underlying pathology, as well as how different automated techniques relate to each other or to nonautomated volumetric quantification methods.

When evaluating a patient with cognitive dysfunction for suspected AD or other neurodegenerative disease, it is important to evaluate for cerebral amyloid angiopathy (CAA) using hemosiderin sensitive sequences (see vascular section). It is worth keeping in mind that, although a majority of patients with AD have some degree of CAA at pathology, [18] not everyone with CAA has AD.[19]

Other Imaging Modalities in AD

Functional imaging generally complements structural imaging in AD diagnosis. Clinical practice has focused on ^{18}F-fluorodeoxyglucose [FDG]-PET and single-photon emission

computed tomography (SPECT), though functional MRI (fMRI) and even magnetoencephalography have elucidated unique associations to pathology and cognitive syndromes.[20,21] Several studies suggest that the spatial patterns of hypometabolism in FDG-PET and hypoperfusion in SPECT overlap with MRI patterns of atrophy, especially in the inferior parietal cortex, lateral temporal cortex, posterior cingulate, and/or the pre-cuneus. [22–24] For older patients, it is unclear if FDG-PET adds diagnostic value beyond structural MRI, though it may be more sensitive in younger AD patients at early disease stages.[25] In our experience, if the clinical syndrome fits AD, but atrophy is not present in expected locations, then FDG-PET or other biomarkers can be helpful for AD diagnosis.

Recent advances in molecular PET (amyloid and tau) are likely to change imaging practices in AD. Molecular PET can verify the distribution of proteinopathies, such as β-amyloid and tau due to AD. Amyloid PET allows for the detection of cortical β-amyloid (Fig. 2A), although the distribution is diffuse across AD variants[26] and does not correlate well with clinical syndromes.[27] Recent work suggests that amyloid positivity in cognitively normal older adults may predict future decline.[28] The recent introduction of tau PET imaging has shown promise in contributing to diagnostic accuracy on the basis of detecting NFT pathology and, furthermore, the distribution of tau tracer uptake correlates with pathologic progression (Fig. 2B).[8,29] One tau PET tracer recently received FDA approval (https:// www.reuters.com/article/brief-cerveau-technologies-announces-fda-idUSASA09U4Q). Despite the clear benefits of molecular PET, current limitations include the need for a specialized PET center and the high cost.

Vascular Dementia

Background

Cerebrovascular disease can cause cognitive impairments that range in severity from mild cognitive impairment to VaD. Vascular cognitive impairment (VCI) is an umbrella term that captures this spectrum of disease, which can result from clinical strokes or subclinical vascular brain injury. VCI can be identified by both neuroimaging and neuropathologic[30] methods, and includes several subtypes, each with its own neuroimaging findings. The most prevalent etiology of VCI is related to alterations in small vessels, which affect the blood–brain barrier and white matter (WM).[31] The subtypes covered here include sporadic small vessel disease (SVD), as well as prototypical examples of sporadic and hereditary protein accumulation vasculopathies, such as Binswanger's disease, amyloid angiopathy, and cerebral autosomal dominant arteriopathy with subcortical infarcts and leukoencephalopathy (CADASIL).

One of the difficulties associated with studying VCI is the frequent overlap of VCI with other pathological entities. Population-based clinicopathological prevalence rates of pure VaD range from ~2% to 24%, and that of mixed AD/VaD from ~4% to 22%.[32,33] Concurrent CVD with neurodegenerative pathology appears to lower the threshold for developing dementia, with the most frequent co-pathologies being AD and/or LBD.[34,35]

Small Vessel Disease and Binswanger's Disease

SVD is the most common cause of VCI. From a clinical perspective, VCI due to SVD is characterized by gradually progressive cognitive impairment, typically in the domains of processing speed and executive functions,[36] as well as motor slowing and changes in balance.[37,38] In addition to small vessel ischemia and hemorrhages, SVD is associated with blood–brain-barrier compromise,[39] a state of chronic cerebral hypoperfusion, and WM degeneration.[40,41]

The "classic" neuroimaging biomarkers of SVD include various types of white matter hyperintensities (WMH)[42] and lacunar infarcts (strokes). The WMHs of vascular etiology can present as multiple punctate or confluent periventricular lesions, leukoaraiosis, and subcortical lesions (Fig. 3A). Lacunar infarcts, characterized by cavitating lesions or lacunes, are typically confined to the WM and subcortical gray matter (GM), and are thought to be on a continuum with WMH as biomarkers of SVD. Understanding factors that determine the location and pattern of WMHs is an area of ongoing research. Importantly, not all periventricular WMHs are due to SVD. For instance, posterior periventricular WMH may be associated with AD neuropathology, rather than typical SVD.[43,44] Additionally, more sensitive imaging modalities such as diffusion MRI have shown that in patients with WMH on FLAIR/T2 images quantifiable diffusion abnormalities can be detected even in regions of normally appearing white matter (NAWM), suggesting a greater area is affected than detected by visual assessment alone.[45]

Novel quantitative biomarkers of SVD include enlarged Virchow–Robin spaces (eVRS) seen on T2 sequences, associated in normal elderly with increased risk of incident dementia.[26] These enlarged fluid-filled spaces line the brain vasculature and have been associated with WMHs, lacunar strokes, as well as MCI-AD (Fig. 3B).[46,47] The centrum semiovale eVRS have been associated with cortical superficial siderosis,[48] whereas diffusely spread eVRS throughout WM has been associated with lobar microhemorrhages.[49] Basal ganglia eVRS, much like deep cortical microbleeds (CMBs), are associated with hypertension. It is hypothesized that eVRS may in part reflect a state of impaired interstitial fluid drainage, associated with small vessel angiopathies due to protein failure elimination, such as CAA, discussed below.[48]

Cortical microinfarcts (CMI) are also emerging as a potential biomarker for SVD (Fig. 3C). Smaller than lacunar infarcts, several autopsy series have shown that CMIs are not only prevalent in individuals with diagnoses of VaD, but also in individuals with AD (~40%) as well as up to $\frac{1}{3}$ of elderly persons without dementia.[50–52] Initially described on 7T MRI,[23] they may also be detectable on high-quality 3T MRI.[52] In addition to the combinatorial effect of general vascular injury burden on cognitive impairment, CMIs may have a unique contribution to cognitive deficits.[52]

Binswanger's disease is considered a prototypical clinical syndrome of VCI. Brain imaging shows progressive confluent subcortical and periventricular WM degeneration on FLAIR/T2, hypoperfusion on SPECT, and hypometabolism on FDG-PET.[36,53] Physiologic neuroimaging techniques, such as dynamic contrast-enhanced MRI (DCE-MRI),[54] for assessing blood–brain barrier integrity in combination with biofluid markers, have shown a

characteristic unrelenting progressive course of hypoxic injury with inflammatory disruption of the blood–brain barrier.[36,55]

Other Imaging Modalities in SVD

Additional quantitative biomarkers of SVD are being investigated to further characterize WM disease, blood–brain barrier disruption, and hypoperfusion. These include diffusion imaging,[56] proton magnetic resonance spectroscopy (1H-MRS), arterial spin labeling (ASL) perfusion,[57] and CO_2 inhalation vascular reactivity.[58] Biomarkers for detection of early subclinical stages of cerebrovascular disease might provide a window for intervention, promising to impact not only VaD but also adverse brain aging as well as neurodegenerative diseases such as AD, for which CVD is a major risk factor.

Cerebral Amyloid Angiopathy

CAA is caused by amyloid deposits in blood vessel walls and is associated with both aging and AD pathology. Neuroimaging in CAA is characterized by CMBs and progressive diffuse WMHs.[41] CMBs can be seen as small MRI signal voids (hypointensities) on susceptibility-weighted imaging (SWI) or T2*-weighted gradient-recalled echo (GRE) (Fig. 3D) caused by microscopic pathological changes such as perivascular deposits of hemosiderin from microhemorrhages (Fig. 3E).[59] In contrast to other disorders associated with the development of microhemorrhage, such as hypertension, CMBs in CAA tend to be peripheral in location, located at the cortical gray–WM interface. Overall, the relationship between CMBs and cognition appears to be nonlinear, with higher counts of CMBs more consistently associated with cognitive impairment.[60]

Hereditary Vasculopathies

A common hereditary cause of vasculopathy is CADASIL.[61,62] It predominantly involves SVD secondary to mutations in the *NOTCH3* gene.[48,63] Mean age of onset of cognitive and motor decline is in the 40s, spanning 30s to 70s, with a high co-prevalence of migraine headaches. Neuroimaging in CADASIL is notable for extensive WM damage including demyelination and lacunar infarctions as well as hemorrhages, often with relatively unique involvement of anterior temporal lobes and insulae (Fig. 3F).[64] A 2015 study on mice carrying *NOTCH3* mutations suggests that pericytes are the first cells affected. An increase in Notch3 aggregation leads to a loss of pericytes, resulting in reduced pericyte coverage of blood vessels, as well as reduced astrocyte polarization, a loss of astrocytic end-foot coverage, a loss of endothelial junction proteins, and leakage of proteins through the blood–brain barrier.[65] Thus, this mutation might act through disruption of the blood–brain barrier and other microvascular dysfunction.[65] Another recently identified set of mutations identified as a relatively common cause of monogenic central nervous system (CNS) vascular disease is the type IV collagen (*COL41A* and *COL41B*) mutations, which often cause multi-system disease.[66–70] These disorders can present with fetal to adult onset. In adults, the pattern of vascular disease often resembles SVD, but features that help with diagnosis include deep intracerebral hemorrhage, periventricular cysts involving subcortical structures, porencephaly, and intracranial aneurysms (Fig. 3G,H).[71–73] In addition to cerebrovascular disease, mutations in these genes are often associated with retinal and renal vascular disease.[69]

Frontotemporal Dementia Spectrum Disorders

When discussing FTD-spectrum disorders, it is important to distinguish between clinical syndromes and pathological entities, as some clinical syndromes can have more than one pathological substrate, and conversely, some pathological entities might present with more than one clinical syndrome. The term FTD often refers to three clinical *syndromes*, behavioral variant frontotemporal dementia (bvFTD) and two types of PPA, the semantic and nonfluent variants of PPA. Given the distinct neuroimaging findings in the nonfluent and semantic variants of PPA, these are discussed in the section on PPA below, together with the logopenic variant of lvPPA (usually due to underlying AD). There are also two motor FTD syndromes: progressive supranuclear palsy syndrome (PSPS) and CBS. When referring to the pathological entities, FTLD refers to a collection of three main *pathological* entities: FTLD-tau, FTLD-TDP (TAR DNA-binding protein) and FTLD-FUS (fused in sarcoma); FTLD-tau subtypes include corticobasal degeneration (CBD), progressive supranuclear palsy (PSP), and Pick's disease (PiD).[74] Below we present the general neuroimaging findings associated with bvFTD (clinical syndrome) as well as different imaging presentations of bvFTD as a function of its underlying FTLD subtype. We also discuss neuroimaging in PSPS and CBS.

Behavioral Variant of FTD

bvFTD is a neurodegenerative disease that affects personality, behavior, and cognition.[75] It is the most common FTD syndrome,[76] with the majority of patients presenting between ages 45 and 64 years of age.[77] Studies suggest that it is the most common or second most common pre-senile dementia.[76,78,79] International consensus criteria for possible bvFTD require three of the following six symptoms to be prominent in the early stages of the disease: disinhibition, apathy, loss of empathy, hyperorality or changes in dietary habits or preferences, simple or complex repetitive movements or behaviors, and a dysexecutive cognitive profile.[75] Probable bvFTD criteria also requires frontal and/or anterior temporal atrophy on MRI or CT, or hypoperfusion/hypometabolism on PET or SPECT.[75] Brain MRI often can help distinguish bvFTD from other neurodegenerative and psychiatric syndromes. [80,81] However, MRI should be interpreted in the context of clinical symptoms, as disproportionate atrophy can be subtle or overlooked (one study reviewing radiology reports for MRI scans in 40 patients subsequently diagnosed clinically with bvFTD found that the correct diagnosis was considered radiologically in only 10% of cases, despite the presence of atrophy considered to be consistent with bvFTD[82]). Atrophy in bvFTD is generally observed in frontotemporal structures including the insula, anterior cingulate, anterior temporal lobes, striatum, amygdala, and thalamus.[83–85] Neuroimaging profiles can vary substantially, however, between patients with bvFTD (Fig. 4).[86]

Pathological Substrates of bvFTD and Neuroimaging

The underlying pathological substrate of bvFTD affects the spatial distribution of atrophy observed on brain MRI. The three common pathological substrates of bvFTD (FTLD-tau, FTLD-TDP, and FTLD-FUS) are each comprised of several subtypes. Tau exists in two forms that result from alternate splicing: a 3 amino-acid sequence repeat form (3R) and a 4-repeat form (4R). The most common tau forms associated with bvFTD are PiD (3R), CBD

(4R), and PSP (4R). Each form of tau pathology usually is associated with a distinct atrophy pattern. For example, PiD has asymmetric frontoinsular atrophy that extends into the anterior temporal lobes and, when severe, has been described as "knife-edge" due to the severe thinning of the gyri.[87] Patients with bvFTD due to CBD, however, show relative preservation of the frontoinsular area, greater dorsal atrophy, and relative sparing of temporal and parietal structures.[88] Despite historical clinical lore, our recent data suggest that bvFTD due to CBD pathology is not consistently associated with asymmetric atrophy. [15,88]

Of the four subtypes of TDP-43 pathology, types A and B are most commonly associated with a bvFTD syndrome.[89] Type A is usually found in patients with progranulin (*PGRN*) mutations (described below).[89] Type B pathology is often associated with FTD motor neuron disease (FTD-MND), and atrophy tends to affect the frontal lobes symmetrically with insular and anteromedial temporal lobe involvement.[86] Finally, FTLD-FUS (usually sporadic) is a very rare pathological cause of bvFTD, often presenting with early onset (20s–40s) with marked psychiatric features and severe caudate atrophy in addition to frontotemporal involvement.[90–92]

Genetic Variants and Imaging

Each genetic variant of bvFTD generally is associated with a neuroimaging phenotype. bvFTD patients with *C9orf72* mutation have a variable age of onset (20s–80s) and often present with psychiatric features including delusions.[93,94] *C9orf72* carriers are less likely to present with language findings than *PGRN* and *MAPT* carriers. MRI in *C9orf72* usually shows symmetric frontotemporal, thalamic, parietal, and cerebellar atrophy, with less medial frontal lobe atrophy than in sporadic bvFTD.[93,95] Patients with *PGRN* mutations usually manifest symptoms around age 60,[96] and have a wide range of clinical phenotypes, including bvFTD, nfvPPA, or CBS.[97] In contrast to *C9orf72* patients, imaging in *PGRN* patients typically shows asymmetric frontotemporal atrophy extending into the parietal lobes with sparing of the cerebellum.[95,98] Patients with *MAPT* mutations usually have earlier symptom onset, often before age 50, with severe temporal lobe atrophy.[99,100] Mutations in *FUS* often cause ALS, but may rarely cause bvFTD.[101]

Other Imaging Modalities in bvFTD

In addition to GM atrophy, bvFTD is also associated with WM abnormalities that have been quantified using volumetric measurements of WM atrophy[102] and changes on diffusion tensor imaging (DTI) metrics.[103,104] One study with 30 bvFTD subjects, 39 AD patients, and 41 cognitively normal controls used DTI to assess WM integrity (WMI), and found alterations in all DTI metrics [i.e., fractional anisotropy (FA), mean diffusivity (MD), radial diffusivity (RD), and axial diffusivity (AD)] in bvFTD compared with controls and AD patients, especially in frontal regions of interest (ROIs). The authors suggested that DTI might add complementary information to volumetric analyses and improve the accuracy of discriminating bvFTD from AD.[105] Furthermore, our own recent data (in revision) suggests that DTI (FA) and ASL perfusion in bvFTD explains additional variance in function and cognition above and beyond atrophy; DTI and ASL studies in pathologically proven cases

are needed. These newer imaging modalities might add to our understanding of the substrates for impairment in bvFTD and possibly help diagnostically as well.

Preliminary evidence suggests that ASL perfusion imaging may help to distinguish bvFTD from other groups with sensitivity and specificity similar to FDG-PET.[106] For example, sensitivity and specificity for ASL to distinguish bvFTD from AD were 83% and 93%, respectively, compared with 89% and 78% for FDG-PET. Although FDG-PET often can be useful in helping to differentiate bvFTD from AD, frontotemporal hypometabolism can occur in frontal variants of AD as well as in primary psychiatric disorders, both of which can clinically resemble bvFTD.[107,108]

There have been some recent exciting advances in the development of PET tracers designed to bind tau paired helical filaments (PHF), allowing one to see in vivo tau distribution. One such tracer that has been the most studied is ^{18}F-AV1451. Very few studies have been conducted in bvFTD at this point. In a few case studies of patients with the *MAPT* mutation, in vivo tracer binding occurs in the expected frontotemporal distribution.[109–111] A caveat is that the specificity of some tau tracers has been questioned, as one leading tracer, ^{18}F-THK5351, has been shown to bind monoamine oxidase B (MAO-B) as well as PHFs.[112]

Corticobasal Syndrome

Consensus diagnostic criteria define CBS by early asymmetrical cortical symptoms including limb rigidity, dystonia or myoclonus, oral buccal or limb apraxia, cortical sensory deficit, and/or alien limb phenomenon.[113] CBS can include language and speech disturbances or begin as a bvFTD syndrome.[114] Atrophy in CBS is typically located in dorsal GM and WM of the posteromedial frontal and perirolandic cortices,[88] as well as the basal ganglia and brainstem.[115]

A difficulty in interpreting the historical literature on imaging findings in CBS is that much was based on cases without pathologically confirmed diagnoses. We now know that CBS can be caused by different pathological entities, each with its own imaging findings, and CBD pathology can present with several clinical phenotypes other than CBS, such as bvFTD, nfvPPA, PSPS, and PCA.[116] In our own center's review of 40 pathologically confirmed cases of CBS, we found at least four common pathologic substrates for this syndrome, including CBD (35%), AD (23%), PSP (13%), and FTLD-TDP (13%);[15] other centers have shown as many as 50% of CBS patients to have PSP pathology on autopsy.[117]

Pathologically confirmed CBD pathology is generally associated with bilateral cortical atrophy in the dorsolateral pre-frontal cortex, supplementary motor area (SMA), perirolandic cortex, striatum, and brainstem.[15] CBD pathology, however, can manifest as several syndromes, each with different neuroimaging signatures that generally adhere to that syndrome's atrophy pattern. For example, nfvPPA due to CBD may present with asymmetric left frontal atrophy. In contrast, CBS due to AD is associated with greater temporoparietal atrophy compared with CBS due to FTLD-TDP or FTLD-tau (including CBD). Regardless of the syndrome, CBD pathology usually affects the perirolandic cortex and striatum.[15,118]

Progressive Supranuclear Palsy

Unlike for CBS which has several pathological correlates, the clinical diagnosis of PSPS has very high correlation with underlying PSP pathology.[117] The classic presentation of PSPS, often referred to as Richardson's syndrome (RS), presents as an atypical parkinsonism with a vertical supranuclear gaze palsy or slowing of vertical saccades, as well as prominent postural instability and falls. PSPS also is often a behavioral disorder; a retrospective review found that 32% of 62 PSPS patients also met criteria for possible bvFTD at their initial assessment.[119]

MRI in PSPS is usually marked by a dilated third ventricle and dorsal midbrain atrophy along the anteroposterior diameter, as well as atrophy of the thalamus, basal ganglia, and insular and frontal cortices.[120,121] Thinning of the superior cerebellar peduncles also is characteristic of this condition.[122] Longitudinal atrophy in the brainstem is at least modestly correlated with clinical progression.[115,123] Midbrain atrophy in PSPS often causes the brainstem to take on a hummingbird-like appearance on sagittal view, referred to as the "hummingbird" or "penguin" sign (Fig. 5).[124] DTI studies have shown that PSPS is associated with widespread alterations in FA and other diffusivity measures in the major WM tracts of the brain, especially the superior cerebellar peduncles.[125–127]

Several methods have been created to capitalize on the anteroposterior midbrain atrophy in PSPS to enhance differential diagnosis, although all are imperfect. One of the possibly more promising indices, although still controversial, multiplies the midsagittal pons/midbrain area ratio by the middle/superior cerebellar peduncle width ratio ("P/M x MCP/SCP ratio"), measured manually. In one study of 33 PSPS, 108 PD, and 19 multiple system atrophy (MSA) clinically diagnosed patients, this index showed 100% sensitivity and specificity in discriminating PSPS from PD and MSA.[128] Another study recently extended the use of this ratio to discriminate PSPS from vascular parkinsonism.[129] This approach is being automated and has shown the ability to distinguish PSPS from PD with comparable accuracy to manually measured ratios.[130] In contrast, measurement of the cerebral peduncle angle (CPA) on axial view does not appear to be reliable in separating pathologically confirmed PSPS cases from CBD, MSA, and LBD.[131]

Some skepticism remains regarding the utility of tau-PET in clinically diagnosed PSPS. Thus far, only a few small studies have been conducted, but it appears that ^{18}F-AV-1451 binding occurs primarily in subcortical structures, including the putamen, globus pallidus, subthalamic nucleus and dentate nucleus, as well as the midbrain, but not the neocortex or WM.[132–134] Although these subcortical regions are affected in PSPS, off-target binding is seen in overlapping regions in neurologically normal controls.[134,135] Postmortem study of ^{18}F-AV-1451 binding in brain tissues suggests that there may be more accurate tracer binding in AD pathology than FTLD-tau.[136] Larger samples with pathological confirmation are required to better estimate the utility of this tracer in PSPS due to FTLD-tau.

Primary Progressive Aphasias

Introduction

The PPAs are a group of three syndromes that share early primary language impairment as the key diagnostic feature: semantic variant PPA (svPPA), nonfluent/agrammatic variant PPA (nfvPPA), and lvPPA. According to the current diagnostic criteria,[137] impaired single-word comprehension and object knowledge are at the crux of the diagnosis of svPPA. In contrast, nfvPPA is characterized by agrammatic language production or effortful, halting speech with impairments in comprehension of complex syntax but spared single-word comprehension and object knowledge. A diagnosis of lvPPA requires impaired single-word retrieval in spontaneous speech and impaired sentence repetition. lvPPA patients often make phonological errors but have spared motor speech, single-word comprehension and grammar. SvPPA and nfvPPA are canonical FTD syndromes typically caused by FTLD pathology. Eighty-three percent of svPPA patients in our institution's brain bank have underlying TDP-43 type C pathology. In contrast, nfvPPA was found to be predominantly (88%) associated with a variety of tauopathies, although the majority were FTLD-4R-tau (CBD or PSP), with a smaller number with PiD, as well as AD and other pathologies such as TDP type A.[138,139] The third PPA, lvPPA, is typically associated with AD pathology.[140,141] These syndromes begin in discrete locations in the brain, and thus patterns of atrophy and hypometabolism on FDG-PET can assist with differential diagnosis, especially early in disease course.[137,142] New research suggests that machine learning algorithms can capitalize on these distinct atrophy patterns to help distinguish between PPA syndromes[143] and possibly even classify the underlying pathological entity.[140] These algorithms are not yet used in clinical practice.

Neuroimaging Patterns in PPA

Atrophy in svPPA begins with asymmetric involvement of the anterior and inferior temporal lobes, typically affecting the left hemisphere first (Fig. 6B).[16,144] As the disease progresses, GM loss extends into the insula, orbitofrontal lobe, anterior cingulate, inferior parietal lobe, medial temporal lobe, basal ganglia, and corresponding areas in the contralateral hemisphere.[144–146] The majority of patients with svPPA have underlying FTLD-TDP type C pathology. svPPA, however, can be associated with FTLD-tau (PiD and globular glial tauopathy), and these cases may have more severe striatal and frontal GM and WM atrophy than FTLD-TDP type C.[140]

In nfvPPA, atrophy usually begins and is most significant in the left inferior frontal lobe, insula, and premotor cortex,[16,144] spreading with disease progression to other perisylvian frontal regions, the temporal lobe, anterior parietal lobe, and subcortical areas such as the caudate, amygdala, thalamus, and cerebellum (Fig. 6A).[146–148] Pathologically confirmed studies of PPAs generally have been limited by small sample sizes, but early studies suggest different atrophy patterns as a function of underlying pathology. A recent study suggested that nfvPPA patients with underlying CBD ($n = 9$) and PSP ($n = 5$) pathology both showed asymmetric frontal atrophy at baseline, but greater overall atrophy was observed in the nfvPPA-CBD group, particularly in the insula and putamen.[139] Additionally, both patient groups showed longitudinal atrophy in the left precentral gyrus and SMA, but the group with

PSP pathology showed a greater amount of volume loss over time, including midbrain atrophy, whereas those with CBD showed significant volume loss in the left anterior prefrontal cortex. nfvPPA-PSP had a higher ratio of WM to GM atrophy at baseline than nfvPPA-CBD.

Structural imaging in lvPPA is marked by volume loss in the left temporoparietal junction, including the middle temporal gyrus and angular gyrus, as well default mode network (DMN) hubs such as the hippocampal formation, posterior cingulate cortex, and precuneus. [140,149] Longitudinally, atrophy in lvPPA encroaches into the anterior and medial temporal lobe, as well as into homologous regions in the opposite hemisphere.[146] Although the majority of lvPPA cases are due to underlying AD pathology, some cohorts have found a subset of patients (0–31%) that are amyloid negative (Aβ-) on PET; these patients might have FTLD-TDP pathology.[140,150,151] Atrophy, WM integrity, and FDG-PET hypometabolism may advance more anteriorly into the anteromedial frontal temporal lobes and medial temporal lobes in the Aβ-cohort, consistent with FTLD pathology.[150,151]

Diffusion Tensor Imaging

Alterations in WM integrity, measured by DTI and tractography, generally appear to recapitulate the patterns of GM atrophy that help distinguish between PPA syndromes, but the extent of WM compromise has consistently been found to extend outside the zone of atrophy,[152–154] although the findings may vary as a function of the specific metric analyzed (i.e., RD versus AD).[155] The utility of DTI as a surrogate of disease progression is being further validated by studies correlating changes in WM integrity with changes in cognitive[156,157] and clinical[158] symptoms in PPA.

svPPA patients have DTI changes in many brain regions (generally more left lateralized), including the uncinate fasciculus, inferior longitudinal fasciculus, corpus callosum, and inferior frontal and orbitofrontal WM.[153,155,159] nfvPPA patients show aberrant WM changes in the left frontal lobes, with involvement of subcortical tracts and the uncinate fasciculus.[156,160] In one study, when DTI metrics were combined with cortical thickness, nfvPPA ($n = 13$) and svPPA ($n = 13$) could be distinguished from each other with a sensitivity of 0.92 and specificity of 0.85.[161] lvPPA patients, however, show broad, bilateral front-temporoparietal WM tract changes[153,159] that are similar to those seen in classic AD. [160] Given the small number of subjects in these studies, the results require validation in larger cohorts.

Dementia with Lewy Bodies and Parkinson's Disease Dementia

Parkinsonian syndromes are often associated with cognitive impairment that can progress to dementia. PDD and dementia with Lewy bodies (DLB) are among the most common neurodegenerative diseases in older adults.[162–164] PDD and DLB share many symptoms, and many consider these disorders to be along a spectrum, although some have argued that these disorders affect different anatomical pathways.[165–167] Pathologically, DLB and PDD are characterized by intraneuronal α-synuclein "Lewy body" inclusions in neurons of the cortex, brainstem, and substantia nigra.[162,168] The primary differentiating feature between PDD and DLB is the timeline of symptom emergence: onset of cognitive symptoms before or within

the same year as onset of motor symptoms warrants a diagnosis of DLB, and motor symptoms that precede cognitive decline by at least a year warrant a PDD diagnosis.[162,165] The central feature of DLB is progressive cognitive decline in executive and visuospatial functions and, usually later in the disease, memory. Other core and associated features include cognitive fluctuations, visual hallucinations, neuroleptic sensitivity, and rapid eye movement (REM) sleep behavior disorder.

Typically considered senile dementias, their incidence increases with above age 65. In light of the increased prevalence of mixed pathologies in elderly, distinguishing DLB from other conditions is complicated by the prevalence of copathologies, with several pathology studies suggesting that ~66% to 77% of clinically diagnosed DLB cases have comorbid DLB and AD pathology (DLB + AD).[169–173]

Brain MRI of patients with DLB may not be diagnostically informative, as patients often have diffuse mild cortical atrophy with no distinct regional pattern. A pathologically confirmed study of 42 DLB cases found that in cases of DLB pathology with low-to-intermediate likelihood of comorbid AD and Braak NFT stage IV ($n = 20$), global atrophy on MRI was not significantly different than controls, with no identified regional patterns, and atrophy was minimal compared with both DLB + AD and AD. In 22 patients with mixed DLB + AD pathology, the spatial distribution of atrophy on MRI generally mapped onto the same areas atrophied in AD and correlated with Braak NFT stage, suggesting that AD pathology drives atrophy in these patients.[174] These findings are in contrast to those of clinically-, rather than pathologically-, diagnosed patients. For example, one voxel-based morphometry (VBM) meta-analysis of 218 DLB clinically diagnosed patients showed reduced right lateral temporal/insular and left lenticular nucleus/insular GM compared with 219 healthy controls.[175] When clinically diagnosed DLB and AD have been compared using VBM analysis, no consistent regions of atrophy differentiated the two, with the possible exception of relatively preserved medial temporal lobe volume in DLB compared with AD.[176–179]

Structural MRI findings in PDD have been variable, though a lack of autopsy-confirmed studies on this topic raises concerns about pathological confounds. A meta-analysis of GM VBM studies comparing clinically diagnosed patients with PDD to healthy controls showed greater volume loss in the medial temporal lobe and basal ganglia in PDD patients.[180] Given pathological comorbidities were not ruled out in this study, it is possible that this finding is reflective of underlying AD rather than α-synuclein pathology. One study based on clinical diagnosis alone suggests that atrophy in PDD is generally similar to DLB,[181] whereas some found slightly less atrophy in PDD compared with DLB,[182,183] which had greater medial temporal volume loss.[183,184] Multiple studies found more atrophy in clinically diagnosed PDD than in PD without dementia;[185,186] again, none have entirely ruled out pathological comorbidities with autopsy of all patients.

DTI in parkinsonian syndromes usually shows decreased WM integrity.[187] DTI has shown promise as a way to distinguish AD from DLB, as clinically diagnosed DLB involves reduced FA in the parieto-occipital WM tracts compared with AD.[188–190] Several studies have observed WM abnormalities in PDD compared with PD and healthy controls as

measured by FA and MD.[191,192] For example, one study of 20 clinical PD patients and 21 clinical PDD patients showed reduced FA in the corpus callosum and the superior longitudinal fasciculus in PDD, and this reduction correlated with Mini-Mental State Examination (MMSE) scores.[193]

Fluorodopa PET and dopamine transporter (DAT) imaging uses the ligand I-fluoropropyl-carbomethoxy-3β-4-iodo-phenyltropane (123I-FP-CIT SPECT or "DaTSCAN") to assess DAT uptake in the nigrostriatal pathway (Fig. 7).[194] The primary utility of DaTSCANs is in differentiating DLB from other nonparkinsonian neurodegenerative disorders, particularly when parkinsonian motor symptoms are absent or subtle in a suspected DLB case and differential diagnosis between DLB and AD is, as a result, especially difficult.[195] One small autopsy-confirmed study of four pure DLB, four DLB with comorbid AD and/or CVD, nine AD (6 had comorbid CVD), and three other neurodegenerative patients (1 CBD, 1 FTLD, and 1 unspecified)[196] found that reduced nigrostriatal DAT uptake was more accurate than clinical diagnosis alone in predicting DLB pathology compared with non-DLB disorders, with a sensitivity of 88% and specificity of 100%.[196] A 2012 meta-analysis that included three studies using clinically diagnosed DLB, as well as the aforementioned autopsy-confirmed study, came to similar conclusions, that DaTSCAN was specific and sensitive in distinguishing DLB from other causes of cognitive impairment: pooled sensitivity was calculated as 86.5%, and pooled specificity was 93.6%.[197] A longitudinal study with 20 clinically diagnosed DLB patients found that DaTSCAN could detect emerging DLB before patients met full clinical criteria.[198] There is some concern about false negatives with DaTSCAN. In one study of 67 clinically diagnosed DLB patients, seven participants had a normal DaTSCAN when first evaluated;[199] five of these seven with normal baseline DaTSCANs were retested and had abnormal scans 9–38 months later. This suggests that a repeat scan may be warranted in cases where DLB is strongly suspected and an initial DaTSCAN is normal.[199] Importantly, DaTSCANs cannot distinguish DLB from PDD or PD, as nigrostriatal DAT uptake is reduced in both disorders.[195,200]

One study of 21 DLB (only 3 pathology-proven) and 21 AD (only 2 pathology-proven) subjects showed that combining FDG-PET with global Pittsburgh compound B (PiB) retention and hippocampal volume greatly increases the ability to discriminate these disorders (area under ROC = 0.98).[201] Another FDG-PET study of 25 patients with clinical AD and 20 with clinical DLB showed that the patients with DLB had greater occipital and posterior temporoparietal hypometabolism, and that this finding could help separate the two conditions, albeit with lower sensitivity (64.3%) and specificity (65.2%) than other clinical information such as informant report of motor coordination or cognitive testing.[202] Despite the promise of techniques such as DaTSCAN, FDG-PET, and PiB PET, they are not yet part of routine clinical care in many places.[203] Other novel ligands that might help identify loss of dopaminergic signaling in vivo are being developed.[203] Attempts to develop PET ligands for α-synuclein have not been successful,[204] but could be helpful in improving the ability to diagnose DLB and PDD earlier and to differentiate them from AD or other neurodegenerative diseases.

Prion Disease and Other Rapidly Progressive Dementias

A RPD is defined as a condition that progresses from first symptom onset to dementia (decline in more than one cognitive domain with functional impairment) in less than 2 years, but the progression often occurs quicker than this.[56] The prototypical causes of RPD are prion diseases (PrD),[205,206] including sporadic (sporadic Jakob–Creutzfeldt disease, sJCD), accounting for 85% of PrD cases, genetic (gPrDs) (10–15% of PrD cases), and acquired (variant and iatrogenic JCD, respectively, vJCD and iJCD, as well as kuru) (1% of cases). [207–209] The genetic forms have been historically classified by their clinicopathological features into three categories: genetic Jakob–Creutzfeldt disease (gJCD), Gerstmann–Sträussler–Scheinker (GSS), and Fatal Familial Insomnia (FFI). It is worth noting, however, that PrDs do not always present rapidly. For instance, within the gPrDs, although FFI and almost all types of fJCD present with a RPD course (fast-progressing gPrD), most GSS patients exhibit a course longer than 3 years and some patients can live for more than a decade (slow-progressing gPrD).[210] A definitive diagnosis of PrD currently requires pathological examination of brain tissue.[211] CSF tests can sometimes be helpful, but most except the new reverse templating quake-induced conversion assay (RT-QuIC) are nonspecific.[212] MRI, however, is fundamental to antemortem diagnosis[205] and sometimes even is useful in differentiating specific etiological and molecular subtypes of sJCD.[213] Unfortunately, the majority of MRIs in patients ultimately shown to have sJCD are misread and the diagnosis is missed in radiology reports.[214]

The quintessential neuroimaging findings associated with sJCD (as well as some other prion diseases) are T2/FLAIR and DWI hyperintensities in the cortex (known as cortical ribboning) and deep GM nuclei, which can be symmetric or asymmetric, with accompanying restricted diffusion on the apparent diffusion coefficient (ADC) map (Fig. 8). [215,216] In sJCD, MRI shows greater sensitivity (91–96%) and specificity (92–94%) than almost any other diagnostic test for differentiating JCD from other RPDs (the RT-QuIC test applied to CSF and olfactory mucosa brushings might be coming close or even exceeding specificity of MRI).[205,216–219] Generally in sJCD, GM hyperintensities on DWI are more evident (brighter) than FLAIR hyperintensities, and they are hypointense on ADC, suggesting restricted diffusion.[215] Sometimes, hypointense cortical ribboning is difficult to see on ADC, but this can be improved with eddy current distortion correction. Unfortunately, this technique often is only available in research settings.[220] The proposed 2017 UCSF Modified JCD MRI criteria for sJCD diagnosis are shown in Table 1, and were modified from previous criteria.[215] DWI hyperintensities generally involve both cortical and subcortical GM (68% of cases), and less frequently the cortex (24%) or basal ganglia (2–5%) alone.[215,217] When considering subcortical involvement in sJCD, the striatum, especially the caudate, seems to be preferentially involved, often with a decreasing anteroposterior gradient of involvement.[221] sJCD can be subclassified into about six "molecular" subtypes based on the molecular weight of protease-resistant prions (type 1 or 2) and on the genotype at the methionine (M)/valine (V) polymorphic codon 129 (MM, MV or VV) in the prion protein gene (PRNP). Some of these subtypes appear to have particular patterns of involvement on MRI, although there is overlap. Knowing the subtype ante

mortem by MRI (as typing requires brain tissue) can help with prognostication of survival and expected symptomatology.[222,223]

Although visual assessment of DWI is critical diagnostically, quantitative approaches to DTI appear to identify more completely the pattern of reduced MD in GM. Our cross-sectional quantitative analyses demonstrated preferential involvement of parietal and temporal lobes, posterior cingulate, thalamus and deep nuclei, generally with less involvement of frontal and occipital lobes.[224] Interestingly, despite the WM involvement in sJCD not generally being appreciated by visual assessment of standard sequences, with DTI analysis we found significant globally reduced WM MD, suggesting possible primary involvement of WM, rather than changes secondary to neuronal degeneration/loss.[225] Given heterogeneous cortical and subcortical involvement across subjects, however, group-wise analyses may underestimate areas of actual brain involvement, even when quantitative assessment is performed, due to the effect of averaging. Currently, single-subject MD quantification experiments are under investigation, with promising results.[226]

Imaging findings in acquired PrDs vary. Dura mater contamination cases appear similar to sJCD, although cases with codon 129 MM have more thalamic involvement. Cadaveric-derived pituitary hormone (often growth hormone) cases might show preferential cerebellar and thalamic involvement compared with most sJCD cases.[227,228] Variant JCD (vJCD) often shows not only cortical involvement but also the "pulvinar sign," in which the pulvinar is brighter than the anterior putamen on DWI and T2-weighted images. Sometimes both the pulvinar and dorsomedial thalamic nuclei are involved, giving the so-called hockey stick sign.[229,230] These thalamic findings, however, can also rarely be found in sJCD,[231,232] as well as in certain infections and metabolic disorders, such as Wernicke's encephalopathy.

Not only do neuroimaging findings in gPrDs vary across the major forms (e.g., gJCD, GSS, and FFI), but also between mutations and even sometimes within families.[210] In gJCD, MRI often resembles sJCD.[208,233,234] In FFI, such prototypical MRI findings of sJCD are usually absent, but can show atrophy.[234–236] In GSS, cerebellar or global atrophy can be found, whereas FLAIR, DWI, and ADC abnormalities are uncommon.[215,235]

Many other conditions other than JCD can present as RPD (Fig. 9). Some nonprion RPD conditions present with MRI findings similar to those seen in JCD. For example, Bartonella encephalopathy, Wilson's disease, Wernicke's encephalopathy, mitochondrial diseases, voltage gated potassium channel (VGKC)-complex antibody-associated dementia,[237–241] and extrapontine myelinolysis,[242,243] may show reduced diffusion in the cortical and subcortical GM. Seizures can also result in DWI cortical ribboning and deep GM nuclei hyperintensities with reduced diffusion;[242] unlike in sJCD, these MRI abnormalities resolve within a few days of seizure control.

With some exceptions, such as those noted above, most non-JCD RPDs do not show reduced diffusion in GM. Many present with prominent FLAIR hyperintensities, such as in antibody-mediated encephalopathies or viral encephali-tides.[244,245] Moreover, such signal alterations often show preferential distribution, such as the patchy medial temporal hyperintensities observed in limbic encephalopathies or the involvement of posterior regions in posterior

reversible encephalopathy syndrome (PRES).[244,246] Finally, the imaging evaluation of an RPD should always incorporate the use of contrast, another helpful tool that can show enhancement in other rapidly progressing conditions such as vasculitis, CNS lymphoma, intravascular lymphoma, and antibody-mediated encephalitides.[205,247] If JCD is being considered and the DWI and ADC scans are unclear diagnostically, consider acquiring b2000 axial and coronal DWI and ADC sequences to better distinguish artifact from true restricted diffusion.[226]

Idiopathic Normal Pressure Hydrocephalus

Idiopathic normal pressure hydrocephalus (iNPH) is a potentially reversible cause of dementia characterized by a combination of clinical and radiographic findings. The clinical presentation of this communicating hydrocephalus includes the triad of cognitive impairment, gait disturbance, and urinary incontinence[248] along with ventriculomegaly on neuroimaging, in the context of normal CSF pressure.[249] Ventriculomegaly, however, is not specific to iNPH and therefore requires the clinician to rule out numerous other causes, such as obstructive hydrocephalus and ventricular enlargement secondary to atrophy (hydrocephalus ex vacuo). iNPH is important to diagnose, because if it is caught early, it is one of the few treatable, if not reversible, dementias.[250,251] If a patient's clinical and neuroimaging features are suggestive of NPH, usually a large-volume (30 or more cc) lumbar puncture (LP) (known as "tap test") and/or a 72-hour lumbar CSF drain trial is performed as a diagnostic test looking for transient symptomatic and objective improvement, mostly in gait and urinary incontinence, to identify subjects most likely to benefit from shunt implantation. Response rates often are in the ~60–80% range, but vary considerably between studies, possibly due to several factors, including the measures used to assess NPH and outcomes.[248,250–253] Because the clinical presentation of iNPH frequently is not specific and diagnostic neuroimaging parameters have suboptimal sensitivity and specificity, the diagnosis of iNPH can be difficult and remains controversial.

One of the greatest challenges in diagnosing iNPH is that no imaging modality has been shown consistently between studies to have high sensitivity and specificity. Two imaging diagnostic indices, the Evans' index (EI) and the callosal angle (CA), often are used as first-line quantitative indicators of ventriculomegaly in iNPH on cross-sectional images.[249] The EI (defined as the ratio between the widest diameter of the frontal horns and the maximum inner diameter of the skull measured in the same axial plane) is a commonly used parameter to quantify ventriculomegaly, although this ratio varies depending on the location and angle of the slice and is thus problematic.[254] International guidelines suggest a threshold of 0.3,[249] whereas some authors recommend a more stringent threshold of 0.33.[255] The EI is also not specific for iNPH, and is increased in patients with atrophy.[256,257] The CA can help to distinguish between iNPH and hydrocephalus ex vacuo. It is measured on a coronal plane at the posterior commissure on a slice that is perpendicular to the anterior/posterior commissure (AC-PC) plane. Patients with iNPH usually have smaller angles, ~50–80°, compared with those with hydrocephalus ex vacuo (~100–120°),[249] such as due to AD and normal aged subjects.[258]

Other structural findings are reported as supportive of iNPH. Focal dilation of cerebral sulci, particularly the Sylvian fissures, together with narrowing/effacing of the high convexity and medial subarachnoid spaces,[259] also referred to as "disproportionately enlarged subarachnoid-space hydrocephalus" (DESH), had a high positive predictive value for diagnosis of iNPH in a sample of 100 patients (nonpathologically proven) from the Japanese SINPHONI cohort.[259] A more recent study of a similar number of subjects found DESH to have high positive predictive value but low negative predictive value (~69% of shunt responders were DESH negative).[251]

In addition to these structural changes, prominent aqueductal flow voids appreciated on T2-weighted imaging are often described in iNPH, in which CSF flow is accelerated.[260] Increased aqueductal CSF flow was found to be a positive predictor of a good response to shunting.[261]

WM abnormalities are commonly observed onT2-weighted images in iNPH.[249] Periventricular hyperintensities (PVH), indicative of transependymal CSF absorption and altered brain water content, are included in the international diagnostic guidelines, though deep white matter changes (DWMC) can also be observed.[249,262] Although neuropathological evidence consistently finds WM involvement in iNPH,[263] the use of WM abnormalities for iNPH diagnosis remains controversial, especially given the high prevalence of ischemic demyelination and infarction in the elderly population. Tullberg et al found that DWMC and PVH did not help accurately differentiate iNPH ($n = 29$) from Binswanger's disease ($n = 17$).[264] DTI is now being studied to further elucidate the role of WM disease in NPH,[265] and initial results suggest that it may assist with differential diagnosis.[266–269]

Other advanced MRI techniques have been proposed together with DTI to go beyond the limits of structural imaging to help diagnose iNPH more accurately. New CSF quantification techniques such as Time-SLIP sequences are being investigated to gain better insight into CSF flow behavior in NPH.[270] The role of functional imaging in NPH is being explored as well: a recent study found DMN connectivity to correlate with the severity of cognitive decline in NPH patients.[271] At present, however, the ideal imaging methodologies for the diagnosis of NPH remain to be determined.

Cerebellar Conditions: Multiple System Atrophy, Spinocerebellar Ataxias, and Huntington's Disease

Cerebellar neurodegenerative diseases are a heterogeneous group of disorders, the most common of which are MSA, the spinocerebellar ataxias (SCAs), and idiopathic cerebellar ataxias (IDCAs).

Multiple System Atrophy

MSA is a progressive neurodegenerative disease characterized pathologically by widespread α-synucleinpositive glial cytoplasmic inclusions in the striatonigral and/or olivopontocerebellar regions. Clinically, MSA presents with a combination of progressive autonomic failure and motor symptoms. When motor symptoms include parkinsonism that is

poorly responsive to levodopa, it is called MSA-parkinsonism or (MSA-P). When the prominent motor features are cerebellar, the syndrome is called MSA-cerebellar (MSA-C). [272] MSA-C and MSA-P likely represent a phenotypic spectrum rather than two distinct syndromes. The diagnostic accuracy of MSA is somewhat low and varies greatly (64–88%), depending on whether the evaluation was performed by a specialist or general neurologist and whether established criteria are used. When applied correctly, particularly by those with knowledge of parkinsonian and cerebellar disorders, the specificity of the MSA clinical criteria to describe the neuropathological findings is quite good (86% to 99%).[273,274]

Imaging biomarkers have been developed in an attempt to differentiate MSA from other parkinsonian and/or cerebellar conditions presenting with similar symptoms. MSA-C often shows the classic "hot cross bun" (HCB) or "cruciform T2" sign, which is characterized by pontomedullary hyperintensity on axial T2/FLAIR and/or proton-density weighted MRI, often with accompanying middle cerebellar peduncle and cerebellar hemisphere hyperintensity (Fig. 10).[275–277] This sign can help differentiate MSA from other parkinsonian syndromes,[276,278,279] but it is neither pathognomonic for MSA-C nor is it always present. As the HCB sign is likely due to gliosis resulting from degeneration of pontine and cerebellar neurons and the traversing pontocerebellar fibers,[275,280] it is also found in other diseases causing olivopontocerebellar atrophy,[275] including SCA1 (21%),[281] SCA2 (64%),[281] SCA3, SCA7, SCA13, SCA17,[282] dentatorubral pallidoluysian atrophy (DRPLA),[283] and very rarely in vJCD[284] and CNS vasculitis.[285] Furthermore, recent studies show that a combination of midbrain, corpus callosum, and cerebellar atrophy occurs more frequently than the "hot cross bun" (HCB) or putaminal rim sign (see below for MSA-P).[286] Several studies have shown that compared with PD and PSP, MSA has significantly greater striatum, brainstem, and cerebellar atrophy.[287–293] One study by Ngai et al suggested that mild MCP FLAIR hyperintensity can also occur in normal individuals independent of age. [294] Proton-density weighted imaging may be more sensitive and allow earlier detection of this sign than standard T2/FLAIR MRI.[277]

The syndrome of MSA-P does not typically demonstrate the HCB sign. Instead, structural imaging may show dorsal putaminal atrophy, putaminal GRE/T2 hypointensity compared with the globus pallidus and red nucleus, and a nonspecific, hypertintense T2 "slit-like" putaminal rim on 1.5T MRI, also known as the "putaminal rim sign."[295,296] Although this latter sign can help distinguish MSA-P from MSA-C and PD, on a 3.0T MRI the putaminal rim sign can be seen in normal 30–60 years olds subjects.[286]

One study using DTI with tract-based spatial statistics (TBSS), found MSA had increased MD in the corticospinal tract, middle and inferior cerebellar peduncles, and medial lemniscus compared with controls.[297] Compared with PD, MSA showed widespread reduced FA and increased MD, and compared with PSP, MSA showed increased MD in the anterior thalamic radiations and superior cerebellar peduncles.[297] Diffusion, PET, and SPECT imaging also have identified abnormalities in MSA-P and MSA-C compared with controls,[287,297–305] and in some studies compared with PD[287,297,306–308] and PSP. [287,297,301,302]

The Spinocerebellar Ataxias

The SCAs are an autosomal-dominantly inherited, clinically diverse group of neurodegenerative disorders featuring progressive cerebellar ataxia, at times with other accompanying signs and/or symptoms. Though all of the SCAs may present with a cerebellar phenotype and accompanying cerebellar atrophy, a few have other clinical and neuroimaging findings. The classic CT or MRI of a SCA patient demonstrates only cerebellar atrophy. The "pure" cerebellar phenotype is seen in SCA variants 5, 6, 8, 10, 11, 14–16, 22, and 26, whereas types 4, 18, 21, 23, 25, and 27 may demonstrate a more complex clinical phenotype also without relatively circumscribed cerebellar atrophy.[38] For example, SCA4, SCA18, SCA23, and SCA25 can present with sensory neuropathy, and SCA 10 may present with epilepsy.[309]

The remaining SCAs can present with other imaging findings, but are also distinguished by their clinical presentation. Brainstem atrophy may be seen in SCA1, 2, 3, 7, and 13.[309] Caudate atrophy may be seen in SCA1 and SCA3, with executive cognitive impairment on neuropsychological testing.[310] Variable cognitive deficits can occur in SCA2, SCA12, SCA17, and SCA19, all of which also demonstrate generalized cerebral atrophy.[283,311] Some SCAs may even present with parkinsonism and/or spasticity, which can make it difficult to distinguish these clinically from MSA, PSP, or hereditary spastic parapareses (HSPs).[312] Though patients with SCA17 usually present with early ataxia or dementia, with or without epilepsy, many patients later show parkinsonism, dystonia, saccadic slowing, hyperreflexia, and/or mutism on examination. SCA3 (i.e., Machado–Joseph disease), probably the most common SCA,[283] may be the most variable in its phenotypic presentation, which can include pure cerebellar ataxia, parkinsonism, spastic paraplegia, neuropathy, impaired temperature sense, pseudoexophthalmos, faciolingual myokymia, dystonia, and/or restless legs syndrome,[313–315] and can present with atrophy of the frontal lobes, temporal lobes, and globus pallidus.[316] SCA7 is distinguished by associated dyschromatopsia and retinal disease (pigmentary macular degeneration).[317]

Other neurodegenerative, autoimmune, and paraneoplastic conditions that can mimic MSA or the SCAs clinically should also be considered in patients presenting with progressive ataxia. IDCAs refer to a group of sporadic disorders of unknown etiology, characterized by the constellation of cerebellar symptoms occurring in late life. Since its original description, [318] many cases of IDCA eventually have been identified as various forms of MSA, SCAs, paraneoplastic disorders, Friedreich's ataxia, fragile-X-associated tremor/ataxia syndrome (FXTAS), and autosomal recessive cerebellar ataxias.[319–321] IDCA associated with parkinsonism has been clinically distinguished from MSA-C by the latter showing the HCB sign with high sensitivity (97%) and specificity (100%).[322] DRPLA presentations vary depending on the age of onset. Early onset cases typically feature ataxia, myoclonus, and epilepsy, whereas late-life presentations have symptoms identical to Huntington's disease (HD).[283,323] Characteristic MRI findings in DRPLA, in addition to brainstem and cerebellar atrophy, are subcortical WM lesions, the latter of which usually are not seen in MSA, HD, or the SCAs.[283] Hypertrophic olivary degeneration is also characteristic of DRPLA.

Friedreich's ataxia can also mimic SCAs clinically. In late stages of disease, MRI can show narrowing of the AP diameter of the cervical spinal cord.[309] The early stages of FXTAS may

resemble MSA both clinically and with T2 hyperintensity in the middle cerebellar peduncles.[257,324,325] Finally, autoimmune and paraneoplastic cerebellar disorders, including anti-Yo or antiglutamic acid decarboxylase antibody syndromes, may present with evidence of subacute inflammation and corresponding cerebellar T2/FLAIR hyperintensity and contrast enhancement, or with chronic cerebellar degeneration on T1-weighted sequences. [326,327]

Huntington's Disease

HD is an autosomal dominant neurodegenerative condition caused by a trinucleotide repeat expansion of CAG in the *huntingtin* gene on chromosome 4 that results in progressive motor, cognitive, and behavioral dysfunction.

The most consistently reported structural neuroimaging finding in HD is striatal atrophy. Longitudinal large cohort studies with hundreds of subjects, such as PREDICT-HD and TRACK-HD, have demonstrated that higher CAG repeat lengths and even premotor HD (pmHD) are associated with faster rates of striatal atrophy.[328–330] Importantly, striatal atrophy can occur before the onset of motor symptoms.[329] In a study from our center of 13 patients with pmHD and 13 age and gender-matched controls, smaller caudate volume combined with quantitative phase measurements on 7T MRI GRE sequences improved the prediction of time to disease onset (disease burden score).[331] Surface-based morphometry with 3T MRI in pmHD subjects with executive dysfunction has shown evidence of anteromedial paraventricular caudate atrophy, supporting prior neuropathological studies, [332,333] and indicating that this imaging measurement may be useful as a very early disease biomarker. In manifest (motor) stages of HD, structural MRI typically demonstrates global volume loss throughout the cerebrum, basal ganglia, brainstem, and cerebellum,[334] though the caudate, putamen, nucleus accumbens, and amygdala remain the most atrophic.

There is increasing evidence that WM volume reduces years before motor symptoms of HD arise,[329,335–338] and loss of WM integrity in the striatum and corpus callosum on voxel-based MRI and DTI is associated with onset, cognitive decline, motor symptoms, and apathy.[339–343] Interestingly, fMRI studies incorporating blood oxygen level-dependent contrast and FDG-PET studies have shown a tendency for corticostriatal–thalamic overactivation/hypermetabolism in early pmHD and corticostriatal underactivation/ hypometabolism in later stages of HD, which suggests that overactivation/hypermetabolism may precede the latter and represent dysfunction and/or compensatory overactivity.[344–350] Additionally, MR spectroscopy has demonstrated that higher levels of myoinositol in the putamen correlate with motor symptoms in 25 patients with pmHD and 30 patients in the early stages of HD.[351]

Emerging Technologies

An exciting era of neuroimaging biomarkers in dementia has begun, in which advances in technology are being met with similar advancements in statistical techniques and computational power. Machine learning algorithms are being utilized to grapple with these data for the purpose of diagnostic decision making. As noted throughout the text, these studies of diagnostic accuracy are critically dependent on pathologically confirmed cases.

Furthermore, longitudinal studies promise to improve the utility of these methods as markers of disease progression. As the availability of longitudinal datasets increases, it becomes possible to define empirically derived ROIs, which may bolster our ability to reliably track disease progression compared with traditional, anatomically defined ROIs.[352,353] At the same time that sophisticated analytic techniques are being developed, investigation of new techniques to quantify critical molecular and cellular neuropathological processes continues. For instance, ongoing efforts are examining the utility of PET ligands sensitive to inflammation, such as the Translocator Protein-18 kDa (TSPO),[354] to supplement the information provided by amyloid and tau-PET tracers discussed above.

Another promising field in neuroimaging is the study of connectomics, which utilizes data from fMRI and/or DWI to quantify relationships between brain regions, often using mathematical models from graph theory, where brain regions are represented as "nodes" and relationships between them as "edges."[355] Higher order cognitive functions are increasingly viewed as emergent properties of discrete large-scale neuronal networks. Furthermore, pathological processes underlying neurodegenerative diseases are thought to have a predilection for, and propagate within, intrinsically vulnerable networks. One methodology for defining and studying these networks is task-free or "resting state" functional neuroimaging (tf-fMRI), which assumes that regions of the brain that show temporal covariations in BOLD signal are coupled in their function.[356] In addition to its role in defining the brain's functional networks, tf-fMRI is being evaluated as a potential early biomarker of degenerative disease.[357,358] The majority of studies thus far have been conducted in AD, which is known to cause altered network connectivity, particularly within the DMN. Functional connectivity shows promise for early detection of AD pathophysiology. For instance, altered DMN connectivity has been observed in cognitively normal individuals at increased risk of AD, based on positive amyloid scans (florbetapir) and in asymptomatic *APOE ε*4 carriers with negative amyloid scans.[357]

DWI data provides an alternative view of brain connectivity using structural, rather than functional relationships. Whereas edges in tf-fMRI data represent the strength of covariation in blood flow between brain regions, in structural connectivity analyses these edges represent the density or number of myelinated neuronal axons between regions.[359] The incremental validity of these metrics over traditional DTI is being evaluated. The study of connectivity in dementia will benefit greatly from endeavors such as the Human Connectome project, which has set out to better define the functional and structural connectome in healthy participants using high resolution acquisition protocols and advanced analytic techniques. Ultimately, the most powerful models of neurodegeneration will combine multimodal neuroimaging techniques with careful phenotyping, as well as molecular and cellular biomarkers of disease with the promise of serving as powerful markers of therapeutic efficacy in future clinical trials.

Conclusion

Neuroimaging modalities improve the diagnosis of dementia, may be important biomarkers for clinical trials, and may offer the ability to improve the antemortem prediction of pathologic entities via several mechanisms. As we gain a greater appreciation for the

specific atrophy patterns associated with specific pathologies, volumetric imaging can lend a role in predicting pathology. Molecular PET imaging is particularly exciting for its potential to bind specific molecular targets that will help elucidate pathology in vivo. Finally, as we gain a greater appreciation for the role of vascular dysfunction and WM pathology across the spectrum of dementing conditions, a variety of imaging techniques are being developed to better appreciate and track these changes.

Acknowledgments

References

1. Crutch SJ, Schott JM, Rabinovici GD, et al. Alzheimer's Association ISTAART Atypical Alzheimer's Disease and Associated Syndromes Professional Interest Area. Consensus classification of posterior cortical atrophy. Alzheimers Dement. 2017; 13(08):870–884. DOI: 10.1016/j.jalz.2017.01.014 [PubMed: 28259709]

2. McKhann GM, Knopman DS, Chertkow H, et al. The diagnosis of dementia due to Alzheimer's disease: recommendations from the National Institute on Aging-Alzheimer's Association workgroups on diagnostic guidelines for Alzheimer's disease. Alzheimers Dement. 2011; 7(03): 263–269. DOI: 10.1016/j.jalz.2011.03.005 [PubMed: 21514250]

3. Sacks CA, Avorn J, Kesselheim AS. The Failure of Solanezumab -How the FDA Saved Taxpayers Billions. N Engl J Med. 2017; 376(18):1706–1708. DOI: 10.1056/NEJMp1701047 [PubMed: 28467878]

4. Seeley WW, Crawford RK, Zhou J, Miller BL, Greicius MD. Neurodegenerative diseases target large-scale human brain networks. Neuron. 2009; 62(01):42–52. [PubMed: 19376066]

5. Ossenkoppele R, Cohn-Sheehy BI, La Joie R, et al. Atrophy patterns in early clinical stages across distinct phenotypes of Alzheimer's disease. Hum Brain Mapp. 2015; 36(11):4421–4437. DOI: 10.1002/hbm.22927 [PubMed: 26260856]

6. Ossenkoppele R, Jansen WJ, Rabinovici GD, et al. Amyloid PET Study Group. Prevalence of amyloid PET positivity in dementia syndromes: a meta-analysis. JAMA. 2015; 313(19):1939–1949. DOI: 10.1001/jama.2015.4669 [PubMed: 25988463]

7. Suemoto CK, Ferretti-Rebustini REL, Rodriguez RD, et al. Neuropathological diagnoses and clinical correlates in older adults in Brazil: a cross-sectional study. Brayne C, ed PLOS Med. 2017; 14(03):e1002267.doi: 10.1371/journal.pmed.1002267

8. Braak H, Thal DR, Ghebremedhin E, Del Tredici K. Stages of the pathologic process in Alzheimer disease: age categories from 1 to 100 years. J Neuropathol Exp Neurol. 2011; 70(11):960–969. DOI: 10.1097/NEN.0b013e318232a379 [PubMed: 22002422]

9. Grinberg LT, Rüb U, Ferretti RE, et al. Brazilian Brain Bank Study Group. The dorsal raphe nucleus shows phosphotau neurofibrillary changes before the transentorhinal region in Alzheimer's disease. A precocious onset? Neuropathol Appl Neurobiol. 2009; 35(04):406–416. DOI: 10.1111/j. 1365-2990.2009.00997.x [PubMed: 19508444]

10. Frisoni GB, Bocchetta M, Chételat G, et al. ISTAART's NeuroImaging Professional Interest Area. Imaging markers for Alzheimer disease: which vs how. Neurology. 2013; 81(05):487–500. DOI: 10.1212/WNL.0b013e31829d86e8 [PubMed: 23897875]

11. Hashimoto M, Yasuda M, Tanimukai S, et al. Apolipoprotein E epsilon 4 and the pattern of regional brain atrophy in Alzheimer's disease. Neurology. 2001; 57(08):1461–1466. [PubMed: 11673590]

12. van de Pol LA, van der Flier WM, Korf ES, Fox NC, Barkhof F, Scheltens P. Baseline predictors of rates of hippocampal atrophy in mild cognitive impairment. Neurology. 2007; 69(15):1491–1497. [PubMed: 17923611]

13. Li B, Shi J, Gutman BA, et al. Alzheimer's Disease Neuroimaging Initiative. Influence of APOE Genotype on Hippocampal Atrophy over Time - An N=1925 Surface-Based ADNI Study. PLoS One. 2016; 11(04):e0152901.doi: 10.1371/journal.pone.0152901 [PubMed: 27065111]

14. Choo IH, Lee DY, Oh JS, et al. Posterior cingulate cortex atrophy and regional cingulum disruption in mild cognitive impairment and Alzheimer's disease. Neurobiol Aging. 2010; 31(05):772–779. DOI: 10.1016/j.neurobiolaging.2008.06.015 [PubMed: 18687503]

15. Lee SE, Rabinovici GD, Mayo MC, et al. Clinicopathological correlations in corticobasal degeneration. Ann Neurol. 2011; 70(02):327–340. DOI: 10.1002/ana.22424 [PubMed: 21823158]

16. Gorno-Tempini ML, Dronkers NF, Rankin KP, et al. Cognition and anatomy in three variants of primary progressive aphasia. Ann Neurol. 2004; 55(03):335–346. DOI: 10.1002/ana.10825 [PubMed: 14991811]

17. Desikan RS, Rafii MS, Brewer JB, Hess CP. An expanded role for neuroimaging in the evaluation of memory impairment. AJNR Am J Neuroradiol. 2013; 34(11):2075–2082. [PubMed: 23764728]

18. Ellis RJ, Olichney JM, Thal LJ, et al. Cerebral amyloid angiopathy in the brains of patients with Alzheimer's disease: the CERAD experience, Part XV. Neurology. 1996; 46(06):1592–1596. DOI: 10.1212/WNL.46.6.1592 [PubMed: 8649554]

19. Yamada M. Cerebral amyloid angiopathy: emerging concepts. J Stroke. 2015; 17(01):17–30. DOI: 10.5853/jos.2015.17.1.17 [PubMed: 25692104]

20. Buckner RL, Snyder AZ, Shannon BJ, et al. Molecular, structural, and functional characterization of Alzheimer's disease: evidence for a relationship between default activity, amyloid, and memory. J Neurosci. 2005; 25(34):7709–7717. [PubMed: 16120771]

21. Karageorgiou E, Lewis SM, McCarten JR, et al. Canonical correlation analysis of synchronous neural interactions and cognitive deficits in Alzheimer's dementia. J Neural Eng. 2012; 9(05): 056003.doi: 10.1088/1741-2560/9/5/056003 [PubMed: 22871558]

22. Minoshima S, Giordani B, Berent S, Frey KA, Foster NL, Kuhl DE. Metabolic reduction in the posterior cingulate cortex in very early Alzheimer's disease. Ann Neurol. 1997; 42(01):85–94. DOI: 10.1002/ana.410420114 [PubMed: 9225689]

23. Jagust W, Thisted R, Devous MDS Sr, et al. SPECT perfusion imaging in the diagnosis of Alzheimer's disease: a clinical-pathologic study. Neurology. 2001; 56(07):950–956. [PubMed: 11294935]

24. Ibáñez V, Pietrini P, Alexander GE, et al. Regional glucose metabolic abnormalities are not the result of atrophy in Alzheimer's disease. Neurology. 1998; 50(06):1585–1593. [Accessed June 4, 2017] http://www.ncbi.nlm.nih.gov/pubmed/9633698. [PubMed: 9633698]

25. Sanchez-Catasus CA, Stormezand GN, van Laar PJ, De Deyn PP, Sanchez MA, Dierckx RA. FDG-PET for Prediction of AD Dementia in Mild Cognitive Impairment. A Review of the State of the Art with Particular Emphasis on the Comparison with Other Neuroimaging Modalities (MRI and Perfusion SPECT). Curr Alzheimer Res. 2017; 14(02):127–142. [PubMed: 27357645]

26. Lehmann M, Ghosh PM, Madison C, et al. Diverging patterns of amyloid deposition and hypometabolism in clinical variants of probable Alzheimer's disease. Brain. 2013; 136(Pt 3):844–858. [PubMed: 23358601]

27. Jansen WJ, Ossenkoppele R, Knol DL, et al. Amyloid Biomarker Study Group. Prevalence of cerebral amyloid pathology in persons without dementia: a meta-analysis. JAMA. 2015; 313(19): 1924–1938. DOI: 10.1001/jama.2015.4668 [PubMed: 25988462]

28. Donohue MC, Sperling RA, Petersen R, Sun CK, Weiner MW, Aisen PS. Alzheimer's Disease Neuroimaging Initiative. Association Between Elevated Brain Amyloid and Subsequent Cognitive Decline Among Cognitively Normal Persons. JAMA. 2017; 317(22):2305–2316. DOI: 10.1001/jama.2017.6669 [PubMed: 28609533]

29. Ossenkoppele R, Schonhaut DR, Schöll M, et al. Tau PET patterns mirror clinical and neuroanatomical variability in Alzheimer's disease. Brain. 2016; 139(Pt 5):1551–1567. [PubMed: 26962052]

30. Gorelick PB, Scuteri A, Black SE, et al. American Heart Association Stroke Council, Council on Epidemiology and Prevention, Council on Cardiovascular Nursing, Council on Cardiovascular Radiology and Intervention, and Council on Cardiovascular Surgery and Anesthesia. Vascular contributions to cognitive impairment and dementia: a statement for healthcare professionals from

the American Heart Association/American Stroke Association. Stroke. 2011; 42(09):2672–2713. DOI: 10.1161/STR.0b013e3182299496 [PubMed: 21778438]

31. Jellinger KA. Pathology and pathogenesis of vascular cognitive impairment-a critical update. Front Aging Neurosci. 2013; 5:17.doi: 10.3389/fnagi.2013.00017 [PubMed: 23596414]

32. Zaccai J, Ince P, Brayne C. Population-based neuropathological studies of dementia: design, methods and areas of investigation–a systematic review. BMC Neurol. 2006; 6:2.doi: 10.1186/1471-2377-6-2 [PubMed: 16401346]

33. Grinberg LT, Nitrini R, Suemoto CK, et al. Prevalence of dementia subtypes in a developing country: a clinicopathological study. Clinics (Sao Paulo). 2013; 68(08):1140–1145. DOI: 10.6061/clinics/2013(08)13 [PubMed: 24037011]

34. Korczyn AD. The complex nosological concept of vascular dementia. J Neurol Sci. 2002; 203–204:3–6.

35. Snowdon DA, Greiner LH, Mortimer JA, Riley KP, Greiner PA, Markesbery WR. Brain infarction and the clinical expression of Alzheimer disease. The Nun Study JAMA. 1997; 277(10):813–817. [PubMed: 9052711]

36. Rosenberg GA, Wallin A, Wardlaw JM, et al. Consensus statement for diagnosis of subcortical small vessel disease. J Cereb Blood Flow Metab. 2016; 36(01):6–25. DOI: 10.1038/jcbfm.2015.172 [PubMed: 26198175]

37. Jokinen H, Gouw AA, Madureira S, et al. LADIS Study Group. Incident lacunes influence cognitive decline: the LADIS study. Neurology. 2011; 76(22):1872–1878. DOI: 10.1212/WNL.0b013e31821d752f [PubMed: 21543730]

38. de Laat KF, Tuladhar AM, van Norden AGW, Norris DG, Zwiers MP, de Leeuw F-E. Loss of white matter integrity is associated with gait disorders in cerebral small vessel disease. Brain. 2011; 134(Pt 1):73–83. DOI: 10.1093/brain/awq343 [PubMed: 21156660]

39. Wardlaw JM, Doubal FN, Valdes-Hernandez M, et al. Blood-brain barrier permeability and long-term clinical and imaging outcomes in cerebral small vessel disease. Stroke. 2013; 44(02):525–527. DOI: 10.1161/STROKEAHA.112.669994 [PubMed: 23233386]

40. Wardlaw JM. Blood-brain barrier and cerebral small vessel disease. J Neurol Sci. 2010; 299(1–2):66–71. doi:10.1016/j. jns.2010.08.042. [PubMed: 20850797]

41. Wardlaw JM, Smith EE, Biessels GJ, et al. STandards for ReportIng Vascular changes on nEuroimaging (STRIVE v1). Neuroimaging standards for research into small vessel disease and its contribution to ageing and neurodegeneration. Lancet Neurol. 2013; 12(08):822–838. DOI: 10.1016/S1474-4422(13)70124-8 [PubMed: 23867200]

42. Hachinski VC, Potter P, Merskey H. Leukoaraiosis. Arch Neurol. 1987; 44(01):21–23. [PubMed: 3800716]

43. Grimmer T, Faust M, Auer F, et al. White matter hyperintensities predict amyloid increase in Alzheimer's disease. Neurobiol Aging. 2012; 33(12):2766–2773. DOI: 10.1016/j.neurobiolaging.2012.01.016 [PubMed: 22410648]

44. Lee S, Viqar F, Zimmerman ME, et al. Dominantly Inherited Alzheimer Network. White matter hyperintensities are a core feature of Alzheimer's disease: evidence from the dominantly inherited Alzheimer network. Ann Neurol. 2016; 79(06):929–939. DOI: 10.1002/ana.24647 [PubMed: 27016429]

45. Lee DY, Fletcher E, Martinez O, et al. Regional pattern of white matter microstructural changes in normal aging, MCI, and AD. Neurology. 2009; 73(21):1722–1728. DOI: 10.1212/WNL.0b013e3181c33afb [PubMed: 19846830]

46. Adams HH, Hilal S, Schwingenschuh P, et al. A priori collaboration in population imaging: The Uniform Neuro-Imaging of Virchow-Robin Spaces Enlargement consortium. Alzheimers Dement (Amst). 2015; 1(04):513–520. DOI: 10.1016/j.dadm.2015.10.004 [PubMed: 27239529]

47. Ramirez J, Berezuk C, McNeely AA, Scott CJ, Gao F, Black SE. Visible Virchow-Robin spaces on magnetic resonance imaging of Alzheimer's disease patients and normal elderly from the Sunnybrook Dementia Study. J Alzheimers Dis. 2015; 43(02):415–424. DOI: 10.3233/JAD-132528 [PubMed: 25096616]

48. Charidimou A, Jaunmuktane Z, Baron JC, et al. White matter perivascular spaces: an MRI marker in pathology-proven cerebral amyloid angiopathy? Neurology. 2014; 82(01):57–62. DOI: 10.1212/01.wnl.0000438225.02729.04 [PubMed: 24285616]

49. Martinez-Ramirez S, Pontes-Neto OM, Dumas AP, et al. Topography of dilated perivascular spaces in subjects from a memory clinic cohort. Neurology. 2013; 80(17):1551–1556. DOI: 10.1212/WNL.0b013e31828f1876 [PubMed: 23553482]

50. van Veluw SJ, Heringa SM, Kuijf HJ, Koek HL, Luijten PR, Biessels GJ. Utrecht Vascular Cognitive Impairment study group. Cerebral cortical microinfarcts at 7Tesla MRI in patients with early Alzheimer's disease. J Alzheimers Dis. 2014; 39(01):163–167. DOI: 10.3233/JAD-131040 [PubMed: 24121967]

51. De Reuck J, Deramecourt V, Auger F, et al. Post-mortem 7. 0-tesla magnetic resonance study of cortical microinfarcts in neurodegenerative diseases and vascular dementia with neuropathological correlates. J Neurol Sci. 2014; 346(1–2):85–89. DOI: 10.1016/j.jns.2014.07.061 [PubMed: 25129206]

52. van Dalen JW, Scuric EE, van Veluw SJ, et al. Cortical micro-infarcts detected in vivo on 3 Tesla MRI: clinical and radiological correlates. Stroke. 2015; 46(01):255–257. DOI: 10.1161/STROKEAHA.114.007568 [PubMed: 25468879]

53. Román GC. Senile dementia of the Binswanger type. A vascular form of dementia in the elderly. JAMA. 1987; 258(13):1782–1788. [PubMed: 3625988]

54. Zhang CE, Wong SM, van de Haar HJ, et al. Blood-brain barrier leakage is more widespread in patients with cerebral small vessel disease. Neurology. 2017; 88(05):426–432. DOI: 10.1212/WNL.0000000000003556 [PubMed: 28031395]

55. Rosenberg GA. Neurological diseases in relation to the blood-brain barrier. J Cereb Blood Flow Metab. 2012; 32(07):1139–1151. DOI: 10.1038/jcbfm.2011.197 [PubMed: 22252235]

56. Baykara E, Gesierich B, Adam R, et al. Alzheimer's Disease Neuroimaging Initiative. A Novel Imaging Marker for Small Vessel Disease Based on Skeletonization of White Matter Tracts and Diffusion Histograms. Ann Neurol. 2016; 80(04):581–592. DOI: 10.1002/ana.24758 [PubMed: 27518166]

57. Yan L, Liu CY, Smith RX, et al. Assessing intracranial vascular compliance using dynamic arterial spin labeling. Neuroimage. 2016; 124(Pt A):433–441. DOI: 10.1016/j.neuroimage.2015.09.008 [PubMed: 26364865]

58. Lu H, Liu P, Yezhuvath U, Cheng Y, Marshall O, Ge Y. MRI mapping of cerebrovascular reactivity via gas inhalation challenges. J Vis Exp. 2014; 52306(94) •••. doi: 10.3791/52306

59. Schrag M, McAuley G, Pomakian J, et al. Correlation of hypointensities in susceptibility-weighted images to tissue histology in dementia patients with cerebral amyloid angiopathy: a postmortem MRI study. Acta Neuropathol. 2010; 119(03):291–302. DOI: 10.1007/s00401-009-0615-z [PubMed: 19937043]

60. Seo SW, Hwa Lee B, Kim EJ, et al. Clinical significance of microbleeds in subcortical vascular dementia. Stroke. 2007; 38(06):1949–1951. DOI: 10.1161/STROKEAHA.106.477315 [PubMed: 17510457]

61. Razvi SSM, Davidson R, Bone I, Muir KW. The prevalence of cerebral autosomal dominant arteriopathy with subcortical infarcts and leucoencephalopathy (CADASIL) in the west of Scotland. J Neurol Neurosurg Psychiatry. 2005; 76(05):739–741. DOI: 10.1136/jnnp.2004.051847 [PubMed: 15834040]

62. Narayan SK, Gorman G, Kalaria RN, Ford GA, Chinnery PF. The minimum prevalence of CADASIL in northeast England. Neurology. 2012; 78(13):1025–1027. DOI: 10.1212/WNL.0b013e31824d586c [PubMed: 22422895]

63. Kalimo H, Ruchoux M-M, Viitanen M, Kalaria RN. CADASIL: a common form of hereditary arteriopathy causing brain infarcts and dementia. Brain Pathol. 2002; 12(03):371–384. [Accessed June 23, 2017] http://www.ncbi.nlm.nih.gov/pubmed/12146805. [PubMed: 12146805]

64. Chabriat, H., Joutel, A., Dichgans, M., Tournier-Lasserve, E., Bousser, M-G. Review CADASIL. www.thelancet.com/neurology 2009;8

65. Ghosh M, Balbi M, Hellal F, Dichgans M, Lindauer U, Plesnila N. Pericytes are involved in the pathogenesis of cerebral autosomal dominant arteriopathy with subcortical infarcts and

leukoencephalopathy. Ann Neurol. 2015; 78(06):887–900. DOI: 10.1002/ana.24512 [PubMed: 26312599]

66. de Vries LS, Mancini GMS. Intracerebral hemorrhage and COL4A1 and COL4A2 mutations, from fetal life into adulthood. Ann Neurol. 2012; 71(04):439–441. DOI: 10.1002/ana.23544 [PubMed: 22447691]

67. Choi JC. Genetics of cerebral small vessel disease. J Stroke. 2015; 17(01):7–16. DOI: 10.5853/jos. 2015.17.1.7 [PubMed: 25692103]

68. Meuwissen MEC, Halley DJJ, Smit LS, et al. The expanding phenotype of COL4A1 and COL4A2 mutations: clinical data on 13 newly identified families and a review of the literature. Genet Med. 2015; 17(11):843–853. DOI: 10.1038/gim.2014.210 [PubMed: 25719457]

69. Vahedi K, Alamowitch S. Clinical spectrum of type IV collagen (COL4A1) mutations: a novel genetic multisystem disease. Curr Opin Neurol. 2011; 24(01):63–68. DOI: 10.1097/WCO. 0b013e32834232c6 [PubMed: 21157337]

70. Weng Y-C, Sonni A, Labelle-Dumais C, et al. COL4A1 mutations in patients with sporadic late-onset intracerebral hemorrhage. Ann Neurol. 2012; 71(04):470–477. DOI: 10.1002/ana.22682 [PubMed: 22522439]

71. Rannikmäe K, Davies G, Thomson PA, et al. METASTROKE Consortium; CHARGE WMH Group; ISGC ICH GWAS Study Collaboration; WMH in Ischemic Stroke GWAS Study Collaboration; International Stroke Genetics Consortium. Common variation in COL4A1/ COL4A2 is associated with sporadic cerebral small vessel disease. Neurology. 2015; 84(09):918–926. DOI: 10.1212/WNL.0000000000001309 [PubMed: 25653287]

72. Volonghi I, Pezzini A, Del Zotto E, et al. Role of COL4A1 in basement-membrane integrity and cerebral small-vessel disease. The COL4A1 stroke syndrome. Curr Med Chem. 2010; 17(13): 1317–1324. [Accessed June 22, 2017] http://www.ncbi.nlm.nih.gov/pubmed/20166936. [PubMed: 20166936]

73. Gould DB, Phalan FC, van Mil SE, et al. Role of COL4A1 in small-vessel disease and hemorrhagic stroke. N Engl J Med. 2006; 354(14):1489–1496. DOI: 10.1056/NEJMoa053727 [PubMed: 16598045]

74. Mann DMA, Snowden JS. Frontotemporal lobar degeneration: Pathogenesis, pathology and pathways to phenotype. Brain Pathol. 2017; doi: 10.1111/bpa.12486

75. Rascovsky K, Hodges JR, Knopman D, et al. Sensitivity of revised diagnostic criteria for the behavioural variant of frontotemporal dementia. Brain. 2011; 134(Pt 9):2456–2477. DOI: 10.1093/ brain/awr179 [PubMed: 21810890]

76. Hogan DB, Jetté N, Fiest KM, et al. The Prevalence and Incidence of Frontotemporal Dementia: a Systematic Review. Can J Neurol Sci. 2016; 43(01, Suppl 1):S96–S109. [PubMed: 27307130]

77. Seltman RE, Matthews BR. Frontotemporal lobar degeneration: epidemiology, pathology, diagnosis and management. CNS Drugs. 2012; 26(10):841–870. DOI: 10.2165/11640070-000000000-00000 [PubMed: 22950490]

78. Knopman DS, Petersen RC, Edland SD, Cha RH, Rocca WA. The incidence of frontotemporal lobar degeneration in Rochester, Minnesota, 1990 through 1994. Neurology. 2004; 62(03):506–508. [Accessed March 22, 2017] http://www.ncbi.nlm.nih.gov/pubmed/14872045. [PubMed: 14872045]

79. Snowden JS, Neary D, Mann DMA. Frontotemporal dementia. Br J Psychiatry. 2002; 180:140–143. [Accessed March 22, 2017] http://www.ncbi.nlm.nih.gov/pubmed/11823324. [PubMed: 11823324]

80. Lanata SC, Miller BL. The behavioural variant frontotemporal dementia (bvFTD) syndrome in psychiatry. J Neurol Neurosurg Psychiatry. 2016; 87(05):501–511. DOI: 10.1136/ jnnp-2015-310697.The [PubMed: 26216940]

81. Lu PH, Mendez MF, Lee GJ, et al. Patterns of brain atrophy in clinical variants of frontotemporal lobar degeneration. Dement Geriatr Cogn Disord. 2013; 35(1–2):34–50. [PubMed: 23306166]

82. Suárez J, Tartaglia MC, Vitali P, et al. Characterizing radiology reports in patients with frontotemporal dementia. Neurology. 2009; 73(13):1073–1074. DOI: 10.1212/WNL. 0b013e3181b9c8a6 [PubMed: 19786700]

83. Schroeter ML, Raczka K, Neumann J, Yves von Cramon D. Towards a nosology for frontotemporal lobar degenerations-a meta-analysis involving 267 subjects. Neuroimage. 2007; 36(03):497–510. DOI: 10.1016/j.neuroimage.2007.03.024 [PubMed: 17478101]

84. Pressman PS, Miller BL. Diagnosis and management of behavioral variant frontotemporal dementia. Biol Psychiatry. 2014; 75(07):574–581. DOI: 10.1016/j.biopsych.2013.11.006 [PubMed: 24315411]

85. Cardenas VA, Boxer AL, Chao LL, et al. Deformation-based morphometry reveals brain atrophy in frontotemporal dementia. Arch Neurol. 2007; 64(06):873–877. DOI: 10.1001/archneur.64.6.873 [PubMed: 17562936]

86. Rohrer JD, Rosen HJ. Neuroimaging in frontotemporal dementia. Int Rev Psychiatry. 2013; 25(02): 221–229. DOI: 10.3109/09540261.2013.778822 [PubMed: 23611351]

87. Murray ME, Kouri N, Lin W-L, Jack CR Jr, Dickson DW, Vemuri P. Clinicopathologic assessment and imaging of tauopathies in neurodegenerative dementias. Alzheimers Res Ther. 2014; 6(01): 1.doi: 10.1186/alzrt231 [PubMed: 24382028]

88. Rankin KP, Mayo MC, Seeley WW, et al. Behavioral variant frontotemporal dementia with corticobasal degeneration pathology: phenotypic comparison to bvFTD with Pick's disease. J Mol Neurosci. 2011; 45(03):594–608. DOI: 10.1007/s12031-011-9615-2 [PubMed: 21881831]

89. Perry, DC., Rosen, HJ. Frontotemporal dementia. In: Geschwind, MD., Racine Belkoura, C., editors. Non-Alzheimer's and Atypical Dementia. West Sussex, UK: John Wiley & Sons, Ltd; 2016. p. 49-63.

90. Lee SE, Seeley WW, Poorzand P, et al. Clinical characterization of bvFTD due to FUS neuropathology. Neurocase. 2012; 18(04):305–317. DOI: 10.1080/13554794.2011.604637 [PubMed: 22060063]

91. Josephs KA, Whitwell JL, Parisi JE, et al. Caudate atrophy on MRI is a characteristic feature of FTLD-FUS. Eur J Neurol. 2010; 17(07):969–975. DOI: 10.1111/j.1468-1331.2010.02975.x [PubMed: 20236174]

92. Snowden JS, Hu Q, Rollinson S, et al. The most common type of FTLD-FUS (aFTLD-U) is associated with a distinct clinical form of frontotemporal dementia but is not related to mutations in the FUS gene. Acta Neuropathol. 2011; 122(01):99–110. DOI: 10.1007/s00401-011-0816-0 [PubMed: 21424531]

93. Sha SJ, Takada LT, Rankin KP, et al. Frontotemporal dementia due to C9ORF72 mutations: clinical and imaging features. Neurology. 2012; 79(10):1002–1011. DOI: 10.1212/WNL. 0b013e318268452e [PubMed: 22875087]

94. Snowden JS, Rollinson S, Thompson JC, et al. Distinct clinical and pathological characteristics of frontotemporal dementia associated with C9ORF72 mutations. Brain. 2012; 135(Pt 3):693–708. DOI: 10.1093/brain/awr355 [PubMed: 22300873]

95. Bocchetta M, Cardoso MJ, Cash DM, Ourselin S, Warren JD, Rohrer JD. Patterns of regional cerebellar atrophy in genetic frontotemporal dementia. Neuroimage Clin. 2016; 11:287–290. DOI: 10.1016/j.nicl.2016.02.008 [PubMed: 26977398]

96. van Swieten JC, Heutink P. Mutations in progranulin (GRN) within the spectrum of clinical and pathological phenotypes of frontotemporal dementia. Lancet Neurol. 2008; 7(10):965–974. DOI: 10.1016/S1474-4422(08)70194-7 [PubMed: 18771956]

97. Rohrer JD, Warren JD. Phenotypic signatures of genetic frontotemporal dementia. Curr Opin Neurol. 2011; 24(06):542–549. DOI: 10.1097/WCO.0b013e32834cd442 [PubMed: 21986680]

98. Whitwell JL, Boeve BF, Weigand SD, et al. Brain atrophy over time in genetic and sporadic frontotemporal dementia: a study of 198 serial magnetic resonance images. Eur J Neurol. 2015; 22(05):745–752. DOI: 10.1111/ene.12675 [PubMed: 25683866]

99. Snowden JS, Adams J, Harris J, et al. Distinct clinical and pathological phenotypes in frontotemporal dementia associated with MAPT, PGRN and C9orf72 mutations. Amyotroph Lateral Scler Frontotemporal Degener. 2015; 16(7–8):497–505. DOI: 10.3109/21678421.2015.1074700 [PubMed: 26473392]

100. Whitwell JL, Jack CR Jr, Boeve BF, et al. Atrophy patterns in IVS10+16, IVS10+3, N279K, S305N, P301L, and V337M MAPT mutations. Neurology. 2009; 73(13):1058–1065. DOI: 10.1212/WNL.0b013e3181b9c8b9 [PubMed: 19786698]

101. Blair IP, Williams KL, Warraich ST, et al. FUS mutations in amyotrophic lateral sclerosis: clinical, pathological, neurophysiological and genetic analysis. J Neurol Neurosurg Psychiatry. 2010; 81(06):639–645. DOI: 10.1136/jnnp.2009.194399 [PubMed: 19965854]

102. Chao LL, Schuff N, Clevenger EM, et al. Patterns of white matter atrophy in frontotemporal lobar degeneration. Arch Neurol. 2007; 64(11):1619–1624. DOI: 10.1001/archneur.64.11.1619 [PubMed: 17998444]

103. Daianu M, Mendez MF, Baboyan VG, et al. An advanced white matter tract analysis in frontotemporal dementia and early-onset Alzheimer's disease. Brain Imaging Behav. 2016; 10(04):1038–1053. DOI: 10.1007/s11682-015-9458-5 [PubMed: 26515192]

104. Mahoney CJA, Simpson IJ, Nicholas JM, et al. Longitudinal diffusion tensor imaging in frontotemporal dementia. Ann Neurol. 2015; 77(01):33–46. [PubMed: 25363208]

105. Möller C, Hafkemeijer A, Pijnenburg YALL, et al. Joint assessment of white matter integrity, cortical and subcortical atrophy to distinguish AD from behavioral variant FTD: a two-center study. Neuroimage Clin. 2015; 9:418–429. [PubMed: 26594624]

106. Tosun D, Schuff N, Rabinovici GD, et al. Diagnostic utility of ASL-MRI and FDG-PET in the behavioral variant of FTD and AD. Ann Clin Transl Neurol. 2016; 3(10):740–751. DOI: 10.1002/acn3.330 [PubMed: 27752510]

107. Vijverberg EGB, Wattjes MP, Dols A, et al. Diagnostic Accuracy of MRI and Additional [18F]FDG-PET for Behavioral Variant Frontotemporal Dementia in Patients with Late Onset Behavioral Changes. J Alzheimers Dis. 2016; 53(04):1287–1297. DOI: 10.3233/JAD-160285 [PubMed: 27372646]

108. Woodward MC, Rowe CC, Jones G, Villemagne VL, Varos TA. Differentiating the frontal presentation of Alzheimer's disease with FDG-PET. J Alzheimers Dis. 2015; 44(01):233–242. DOI: 10.3233/JAD-141110 [PubMed: 25261443]

109. Spina S, Schonhaut DR, Boeve BF, et al. Frontotemporal dementia with the V337M MAPT mutation: Tau-PET and pathology correlations. Neurology. 2017; 88(08):758–766. DOI: 10.1212/WNL.0000000000003636 [PubMed: 28130473]

110. Smith R, Puschmann A, Schöll M, et al. 18F-AV-1451 tau PET imaging correlates strongly with tau neuropathology in MAPT mutation carriers. Brain. 2016; 139(Pt 9):2372–2379. DOI: 10.1093/brain/aww163 [PubMed: 27357347]

111. Bevan Jones WR, Cope TE, Passamonti L, et al. [(18)F]AV-1451 PET in behavioral variant frontotemporal dementia due to MAPT mutation. Ann Clin Transl Neurol. 2016; 3(12):940–947. DOI: 10.1002/acn3.366 [PubMed: 28097206]

112. Ng KP, Pascoal TA, Mathotaarachchi S, et al. Monoamine oxidase B inhibitor, selegiline, reduces (18)F-THK5351 uptake in the human brain. Alzheimers Res Ther. 2017; 9(01):25.doi: 10.1186/s13195-017-0253-y [PubMed: 28359327]

113. Armstrong MJ, Litvan I, Lang AE, et al. Criteria for the diagnosis of corticobasal degeneration. Neurology. 2013; 80(05):496–503. DOI: 10.1212/WNL.0b013e31827f0fd1 [PubMed: 23359374]

114. Kertesz A, Martinez-Lage P, Davidson W, Munoz DG. The corticobasal degeneration syndrome overlaps progressive aphasia and frontotemporal dementia. Neurology. 2000; 55(09):1368–1375. [Accessed March 1, 2017] http://www.ncbi.nlm.nih.gov/pubmed/11087783. [PubMed: 11087783]

115. Dutt S, Binney RJ, Heuer HW, et al. AL-108-231 investigators. Progression of brain atrophy in PSP and CBS over 6 months and 1 year. Neurology. 2016; 87(19):2016–2025. DOI: 10.1212/WNL.0000000000003305 [PubMed: 27742814]

116. Kouri N, Whitwell JL, Josephs KA, Rademakers R, Dickson DW. Corticobasal degeneration: a pathologically distinct 4R tauopathy. Nat Rev Neurol. 2011; 7(05):263–272. DOI: 10.1038/nrneurol.2011.43 [PubMed: 21487420]

117. Josephs KA, Petersen RC, Knopman DS, et al. Clinicopathologic analysis of frontotemporal and corticobasal degenerations and PSP. Neurology. 2006; 66(01):41–48. DOI: 10.1212/01.wnl.0000191307.69661.c3 [PubMed: 16401843]

118. Whitwell JL, Jack CR Jr, Boeve BF, et al. Imaging correlates of pathology in corticobasal syndrome. Neurology. 2010; 75(21):1879–1887. DOI: 10.1212/WNL.0b013e3181feb2e8 [PubMed: 21098403]

119. Kobylecki C, Jones M, Thompson JC, et al. Cognitive-behavioural features of progressive supranuclear palsy syndrome overlap with frontotemporal dementia. J Neurol. 2015; 262(04): 916–922. DOI: 10.1007/s00415-015-7657-z [PubMed: 25663411]

120. Shi HC, Zhong JG, Pan PL, et al. Gray matter atrophy in progressive supranuclear palsy: meta-analysis of voxel-based morphometry studies. Neurol Sci. 2013; 34(07):1049–1055. DOI: 10.1007/s10072-013-1406-9 [PubMed: 23543378]

121. Josephs KA, Whitwell JL, Dickson DW, et al. Voxel-based morphometry in autopsy proven PSP and CBD. Neurobiol Aging. 2008; 29(02):280–289. DOI: 10.1016/j.neurobiolaging.2006.09.019 [PubMed: 17097770]

122. Nicoletti G, Caligiuri ME, Cherubini A, et al. A Fully Automated, Atlas-Based Approach for Superior Cerebellar Peduncle Evaluation in Progressive Supranuclear Palsy Phenotypes. AJNR Am J Neuroradiol. 2017; 38(03):523–530. DOI: 10.3174/ajnr.A5048 [PubMed: 28034996]

123. Tsai RM, Lobach I, Bang J, et al. AL-108–231 Investigators. Clinical correlates of longitudinal brain atrophy in progressive supra-nuclear palsy. Parkinsonism Relat Disord. 2016; 28:29–35. DOI: 10.1016/j.parkreldis.2016.04.006 [PubMed: 27132501]

124. Kim YE, Kang SY, Ma H-I, Ju Y-S, Kim YJ. A Visual Rating Scale for the Hummingbird Sign with Adjustable Diagnostic Validity. J Parkinsons Dis. 2015; 5(03):605–612. DOI: 10.3233/JPD-150537 [PubMed: 26406141]

125. Worker, A., Blain, C., Jarosz, J., et al. Diffusion Tensor Imaging of Parkinson's Disease, Multiple System Atrophy and Progressive Supranuclear Palsy: A Tract-Based Spatial Statistics Study. In: Kassubek, J., editor. PLoS One. Vol. 9. 2014. p. e112638

126. Agosta F, Galantucci S, Svetel M, et al. Clinical, cognitive, and behavioural correlates of white matter damage in progressive supranuclear palsy. J Neurol. 2014; 261(05):913–924. [PubMed: 24599641]

127. Whitwell JL, Avula R, Master A, et al. Disrupted thalamocortical connectivity in PSP: a resting-state fMRI, DTI, and VBM study. Parkinsonism Relat Disord. 2011; 17(08):599–605. DOI: 10.1016/j.parkreldis.2011.05.013 [PubMed: 21665514]

128. Quattrone A, Nicoletti G, Messina D, et al. MR imaging index for differentiation of progressive supranuclear palsy from Parkinson disease and the Parkinson variant of multiple system atrophy. Radiology. 2008; 246(01):214–221. DOI: 10.1148/radiol.2453061703 [PubMed: 17991785]

129. Kim BC, Choi S-M, Choi K-H, et al. MRI measurements of brainstem structures in patients with vascular parkinsonism, progressive supranuclear palsy, and Parkinson's disease. Neurol Sci. 2017; 38(04):627–633. DOI: 10.1007/s10072-017-2812-1 [PubMed: 28078564]

130. Nigro S, Arabia G, Antonini A, et al. Magnetic Resonance Parkinsonism Index: diagnostic accuracy of a fully automated algorithm in comparison with the manual measurement in a large Italian multicentre study in patients with progressive supra-nuclear palsy. Eur Radiol. 2017; 27(06):2665–2675. DOI: 10.1007/s00330-016-4622-x [PubMed: 27761709]

131. Tipton PW, Konno T, Broderick DF, Dickson DW, Wszolek ZK. Cerebral peduncle angle: unreliable in differentiating progressive supranuclear palsy from other neurodegenerative diseases. Parkinsonism Relat Disord. 2016; 32:31–35. DOI: 10.1016/j.parkreldis.2016.08.009 [PubMed: 27553513]

132. Smith R, Schain M, Nilsson C, et al. Increased basal ganglia binding of (18) F-AV-1451 in patients with progressive supra-nuclear palsy. Mov Disord. 2017; 32(01):108–114. DOI: 10.1002/mds.26813 [PubMed: 27709757]

133. Cho H, Choi JY, Hwang MS, et al. Subcortical (18) F-AV-1451 binding patterns in progressive supranuclear palsy. Mov Disord. 2017; 32(01):134–140. DOI: 10.1002/mds.26844 [PubMed: 27813160]

134. Passamonti L, Vázquez Rodríguez P, Hong YT, et al. 18F-AV-1451 positron emission tomography in Alzheimer's disease and progressive supranuclear palsy. Brain. 2017; 140(03):781–791. DOI: 10.1093/brain/aww340 [PubMed: 28122879]

135. Coakeley S, Cho SS, Koshimori Y, et al. Positron emission tomography imaging of tau pathology in progressive supranuclear palsy. J Cereb Blood Flow Metab. 2017; 37(09):3150–3160. [PubMed: 28155586]

136. Marquié M, Normandin MD, Meltzer AC, et al. Pathological correlations of [F-18]-AV-1451 imaging in non-alzheimer tauopathies. Ann Neurol. 2017; 81(01):117–128. DOI: 10.1002/ana. 24844 [PubMed: 27997036]

137. Gorno-Tempini ML, Hillis AE, Weintraub S, et al. Classification of primary progressive aphasia and its variants. Neurology. 2011; 76(11):1006–1014. DOI: 10.1212/WNL.0b013e31821103e6 [PubMed: 21325651]

138. Spinelli EG, Mandelli ML, et al. Typical and atypical pathology in primary progressive aphasia variants. Ann Neurol. 2017; 81:430–443. [PubMed: 28133816]

139. Santos-Santos MA, Mandelli ML, Binney RJ, et al. Features of Patients With Nonfluent/Agrammatic Primary Progressive Aphasia With Underlying Progressive Supranuclear Palsy Pathology or Corticobasal Degeneration. JAMA Neurol. 2016; 73(06):733–742. DOI: 10.1001/jamaneurol.2016.0412 [PubMed: 27111692]

140. Spinelli EG, Mandelli ML, Miller ZA, et al. Typical and atypical pathology in primary progressive aphasia variants. Ann Neurol. 2017; 81(03):430–443. DOI: 10.1002/ana.24885 [PubMed: 28133816]

141. Harris JM, Gall C, Thompson JC, et al. Classification and pathology of primary progressive aphasia. Neurology. 2013; 81(21):1832–1839. DOI: 10.1212/01.wnl.0000436070.28137.7b [PubMed: 24142474]

142. Rabinovici GD, Jagust WJ, Furst AJ, et al. Abeta amyloid and glucose metabolism in three variants of primary progressive aphasia. Ann Neurol. 2008; 64(04):388–401. DOI: 10.1002/ana. 21451 [PubMed: 18991338]

143. Bisenius S, Mueller K, Diehl-Schmid J, et al. FTLDc study group. Predicting primary progressive aphasias with support vector machine approaches in structural MRI data. Neuroimage Clin. 2017; 14:334–343. [PubMed: 28229040]

144. Rohrer JD, Warren JD, Modat M, et al. Patterns of cortical thinning in the language variants of frontotemporal lobar degeneration. Neurology. 2009; 72(18):1562–1569. DOI: 10.1212/WNL. 0b013e3181a4124e [PubMed: 19414722]

145. Brambati SM, Rankin KP, Narvid J, et al. Atrophy progression in semantic dementia with asymmetric temporal involvement: a tensor-based morphometry study. Neurobiol Aging. 2009; 30(01):103–111. DOI: 10.1016/j.neurobiolaging.2007.05.014 [PubMed: 17604879]

146. Brambati SM, Amici S, Racine CA, et al. Longitudinal gray matter contraction in three variants of primary progressive aphasia: a tenser-based morphometry study. Neuroimage Clin. 2015; 8:345–355. DOI: 10.1016/j.nicl.2015.01.011 [PubMed: 26106560]

147. Rogalski E, Cobia D, Harrison TM, Wieneke C, Weintraub S, Mesulam M-M. Progression of language decline and cortical atrophy in subtypes of primary progressive aphasia. Neurology. 2011; 76(21):1804–1810. DOI: 10.1212/WNL.0b013e31821ccd3c [PubMed: 21606451]

148. Gorno-Tempini ML, Murray RC, Rankin KP, Weiner MW, Miller BL. Clinical, cognitive and anatomical evolution from nonfluent progressive aphasia to corticobasal syndrome: a case report. Neurocase. 2004; 10(06):426–436. DOI: 10.1080/13554790490894011 [PubMed: 15788282]

149. Greicius MD, Kimmel DL. Neuroimaging insights into network-based neurodegeneration. Curr Opin Neurol. 2012; 25(06):727–734. DOI: 10.1097/WCO.0b013e32835a26b3 [PubMed: 23108250]

150. Whitwell JL, Duffy JR, Strand EA, et al. Clinical and neuroimaging biomarkers of amyloid-negative logopenic primary progressive aphasia. Brain Lang. 2015; 142:45–53. DOI: 10.1016/j.bandl.2015.01.009 [PubMed: 25658633]

151. Matías-Guiu JA, Cabrera-Martín MN, Moreno-Ramos T, et al. Amyloid and FDG-PET study of logopenic primary progressive aphasia: evidence for the existence of two subtypes. J Neurol. 2015; 262(06):1463–1472. DOI: 10.1007/s00415-015-7738-z [PubMed: 25860346]

152. Mahoney CJ, Downey LE, Ridgway GR, et al. Longitudinal neuroimaging and neuropsychological profiles of frontotemporal dementia with C9ORF72 expansions. Alzheimers Res Ther. 2012; 4(05):41.doi: 10.1186/alzrt144 [PubMed: 23006986]

153. Agosta F, Scola E, Canu E, et al. White matter damage in frontotemporal lobar degeneration spectrum. Cereb Cortex. 2012; 22(12):2705–2714. DOI: 10.1093/cercor/bhr288 [PubMed: 21988828]

154. Agosta F, Galantucci S, Magnani G, et al. MRI signatures of the frontotemporal lobar degeneration continuum. Hum Brain Mapp. 2015; 36(07):2602–2614. DOI: 10.1002/hbm.22794 [PubMed: 25821176]

155. Schwindt GC, Graham NL, Rochon E, et al. Whole-brain white matter disruption in semantic and nonfluent variants of primary progressive aphasia. Hum Brain Mapp. 2013; 34(04):973–984. DOI: 10.1002/hbm.21484 [PubMed: 22109837]

156. Mandelli ML, Caverzasi E, Binney RJ, et al. Frontal white matter tracts sustaining speech production in primary progressive aphasia. J Neurosci. 2014; 34(29):9754–9767. DOI: 10.1523/JNEUROSCI.3464-13.2014 [PubMed: 25031413]

157. Charles D, Olm C, Powers J, et al. Grammatical comprehension deficits in non-fluent/agrammatic primary progressive aphasia. J Neurol Neurosurg Psychiatry. 2014; 85(03):249–256. DOI: 10.1136/jnnp-2013-305749 [PubMed: 24039027]

158. D'Anna L, Mesulam MM, Thiebaut de Schotten M, et al. Frontotemporal networks and behavioral symptoms in primary progressive aphasia. Neurology. 2016; 86(15):1393–1399. DOI: 10.1212/WNL.0000000000002579 [PubMed: 26992858]

159. Tu S, Leyton CE, Hodges JR, Piguet O, Hornberger M. Divergent Longitudinal Propagation of White Matter Degradation in Logopenic and Semantic Variants of Primary Progressive Aphasia. J Alzheimer's Dis. 2015; 49(03):853–861. DOI: 10.3233/JAD-150626

160. Mahoney CJ, Malone IB, Ridgway GR, et al. White matter tract signatures of the progressive aphasias. Neurobiol Aging. 2013; 34(06):1687–1699. DOI: 10.1016/j.neurobiolaging.2012.12.002 [PubMed: 23312804]

161. Agosta F, Ferraro PM, Canu E, et al. Differentiation between Subtypes of Primary Progressive Aphasia by Using Cortical Thickness and Diffusion-Tensor MR Imaging Measures. Radiology. 2015; 276(01):219–227. DOI: 10.1148/radiol.15141869 [PubMed: 25734554]

162. McKeith IG. Consensus guidelines for the clinical and pathologic diagnosis of dementia with Lewy bodies (DLB): report of the Consortium on DLB International Workshop. J Alzheimers Dis. 2006; 9(3, Suppl):417–423. [PubMed: 16914880]

163. Aarsland D, Rongve A, Nore SP, et al. Frequency and case identification of dementia with Lewy bodies using the revised consensus criteria. Dement Geriatr Cogn Disord. 2008; 26(05):445–452. DOI: 10.1159/000165917 [PubMed: 18974647]

164. Hogan DB, Fiest KM, Roberts JI, et al. The Prevalence and Incidence of Dementia with Lewy Bodies: a Systematic Review. Can J Neurol Sci. 2016; 43(Suppl 1):S83–S95. DOI: 10.1017/cjn.2016.2 [PubMed: 27307129]

165. Gomperts SN. Lewy Body Dementias: Dementia With Lewy Bodies and Parkinson Disease Dementia. Continuum (Minneap Minn). 2016; 22(2 Dementia):435–463. [PubMed: 27042903]

166. Borroni B, Premi E, Formenti A, et al. Structural and functional imaging study in dementia with Lewy bodies and Parkinson's disease dementia. Parkinsonism Relat Disord. 2015; 21(09):1049–1055. DOI: 10.1016/j.parkreldis.2015.06.013 [PubMed: 26109553]

167. Ballard C, Ziabreva I, Perry R, et al. Differences in neuropathologic characteristics across the Lewy body dementia spectrum. Neurology. 2006; 67(11):1931–1934. DOI: 10.1212/01.wnl.0000249130.63615.cc [PubMed: 17159096]

168. Emre M. What causes mental dysfunction in Parkinson's disease? Mov Disord. 2003; 18(Suppl 6):S63–S71. DOI: 10.1002/mds.10565

169. Schneider JA, Arvanitakis Z, Bang W, Bennett DA. Mixed brain pathologies account for most dementia cases in community-dwelling older persons. Neurology. 2007; 69(24):2197–2204. DOI: 10.1212/01.wnl.0000271090.28148.24 [PubMed: 17568013]

170. Barker WW, Luis CA, Kashuba A, et al. Relative frequencies of Alzheimer disease, Lewy body, vascular and frontotemporal dementia, and hippocampal sclerosis in the State of Florida Brain Bank. Alzheimer Dis Assoc Disord. 2002; 16(04):203–212. [PubMed: 12468894]

171. Walker L, McAleese KE, Thomas AJ, et al. Neuropathologically mixed Alzheimer's and Lewy body disease: burden of pathological protein aggregates differs between clinical phenotypes. Acta Neuropathol. 2015; 129(05):729–748. DOI: 10.1007/s00401-015-1406-3 [PubMed: 25758940]

172. Kraybill ML, Larson EB, Tsuang DW, et al. Cognitive differences in dementia patients with autopsy-verified AD, Lewy body pathology, or both. Neurology. 2005; 64(12):2069–2073. DOI: 10.1212/01.WNL.0000165987.89198.65 [PubMed: 15985574]

173. Irwin DJ, Grossman M, Weintraub D, et al. Neuropathological and genetic correlates of survival and dementia onset in synucleinopathies: a retrospective analysis. Lancet Neurol. 2017; 16(01): 55–65. DOI: 10.1016/S1474-4422(16)30291-5 [PubMed: 27979356]

174. Nedelska Z, Ferman TJ, Boeve BF, et al. Pattern of brain atrophy rates in autopsy-confirmed dementia with Lewy bodies. Neurobiol Aging. 2015; 36(01):452–461. DOI: 10.1016/j.neurobiolaging.2014.07.005 [PubMed: 25128280]

175. Zhong J, Pan P, Dai Z, Shi H. Voxelwise meta-analysis of gray matter abnormalities in dementia with Lewy bodies. Eur J Radiol. 2014; 83(10):1870–1874. DOI: 10.1016/j.ejrad.2014.06.014 [PubMed: 25043498]

176. Watson R, O'Brien JT, Barber R, Blamire AM. Patterns of gray matter atrophy in dementia with Lewy bodies: a voxel-based morphometry study. Int Psychogeriatr. 2012; 24(04):532–540. DOI: 10.1017/S1041610211002171 [PubMed: 22126938]

177. Burton EJ, Karas G, Paling SM, et al. Patterns of cerebral atrophy in dementia with Lewy bodies using voxel-based morphometry. Neuroimage. 2002; 17(02):618–630. [PubMed: 12377138]

178. Whitwell JL, Weigand SD, Shiung MM, et al. Focal atrophy in dementia with Lewy bodies on MRI: a distinct pattern from Alzheimer's disease. Brain. 2007; 130(Pt 3):708–719. DOI: 10.1093/brain/awl388 [PubMed: 17267521]

179. Brenneis C, Wenning GK, Egger KE, et al. Basal forebrain atrophy is a distinctive pattern in dementia with Lewy bodies. Neuroreport. 2004; 15(11):1711–1714. [PubMed: 15257132]

180. Pan PL, Shi HC, Zhong JG, et al. Gray matter atrophy in Parkinson's disease with dementia: evidence from meta-analysis of voxel-based morphometry studies. Neurol Sci. 2013; 34(05):613–619. DOI: 10.1007/s10072-012-1250-3 [PubMed: 23184330]

181. Burton EJ, McKeith IG, Burn DJ, Williams ED, O'Brien JT. Cerebral atrophy in Parkinson's disease with and without dementia: a comparison with Alzheimer's disease, dementia with Lewy bodies and controls. Brain. 2004; 127(Pt 4):791–800. DOI: 10.1093/brain/awh088 [PubMed: 14749292]

182. Beyer MK, Larsen JP, Aarsland D. Gray matter atrophy in Parkinson disease with dementia and dementia with Lewy bodies. Neurology. 2007; 69(08):747–754. DOI: 10.1212/01.wnl.0000269666.62598.1c [PubMed: 17709706]

183. Tam CWC, Burton EJ, McKeith IG, Burn DJ, O'Brien JT. Temporal lobe atrophy on MRI in Parkinson disease with dementia: a comparison with Alzheimer disease and dementia with Lewy bodies. Neurology. 2005; 64(05):861–865. DOI: 10.1212/01.WNL.0000153070.82309.D4 [PubMed: 15753423]

184. Kenny ER, Burton EJ, O'Brien JT. A volumetric magnetic resonance imaging study of entorhinal cortex volume in dementia with lewy bodies. A comparison with Alzheimer's disease and Parkinson's disease with and without dementia. Dement Geriatr Cogn Disord. 2008; 26(03):218–225. DOI: 10.1159/000153432 [PubMed: 18781072]

185. Burton EJ, McKeith IG, Burn DJ, O'Brien JT. Brain atrophy rates in Parkinson's disease with and without dementia using serial magnetic resonance imaging. Mov Disord. 2005; 20(12):1571–1576. DOI: 10.1002/mds.20652 [PubMed: 16116613]

186. Summerfield C, Junqué C, Tolosa E, et al. Structural brain changes in Parkinson disease with dementia: a voxel-based morphometry study. Arch Neurol. 2005; 62(02):281–285. DOI: 10.1001/archneur.62.2.281 [PubMed: 15710857]

187. Cochrane CJ, Ebmeier KP. Diffusion tensor imaging in parkinsonian syndromes: a systematic review and meta-analysis. Neurology. 2013; 80(09):857–864. DOI: 10.1212/WNL.0b013e318284070c [PubMed: 23439701]

188. Watson R, Blamire AM, Colloby SJ, et al. Characterizing dementia with Lewy bodies by means of diffusion tensor imaging. Neurology. 2012; 79(09):906–914. DOI: 10.1212/WNL.0b013e318266fc51 [PubMed: 22895591]

189. Kiuchi K, Morikawa M, Taoka T, et al. White matter changes in dementia with Lewy bodies and Alzheimer's disease: a tractography-based study. J Psychiatr Res. 2011; 45(08):1095–1100. DOI: 10.1016/j.jpsychires.2011.01.011 [PubMed: 21315376]

190. Nedelska Z, Schwarz CG, Boeve BF, et al. White matter integrity in dementia with Lewy bodies: a voxel-based analysis of diffusion tensor imaging. Neurobiol Aging. 2015; 36(06):2010–2017. DOI: 10.1016/j.neurobiolaging.2015.03.007 [PubMed: 25863527]

191. Chen B, Fan GG, Liu H, Wang S. Changes in anatomical and functional connectivity of Parkinson's disease patients according to cognitive status. Eur J Radiol. 2015; 84(07):1318–1324. DOI: 10.1016/j.ejrad.2015.04.014 [PubMed: 25963506]

192. Perea RD, Rada RC, Wilson J, et al. A Comparative White Matter Study with Parkinson's disease, Parkinson's Disease with Dementia and Alzheimer's Disease. J Alzheimer's Dis Park. 2013; 3:123.doi: 10.4172/2161-0460.1000123

193. Kamagata K, Motoi Y, Tomiyama H, et al. Relationship between cognitive impairment and white-matter alteration in Parkin-son's disease with dementia: tract-based spatial statistics and tract-specific analysis. Eur Radiol. 2013; 23(07):1946–1955. DOI: 10.1007/s00330-013-2775-4 [PubMed: 23404139]

194. Booij J, Tissingh G, Boer GJ, et al. [123I]FP-CIT SPECT shows a pronounced decline of striatal dopamine transporter labelling in early and advanced Parkinson's disease. J Neurol Neurosurg Psychiatry. 1997; 62(02):133–140. [Accessed June 22, 2017] http://www.ncbi.nlm.nih.gov/pubmed/9048712. [PubMed: 9048712]

195. Del Sole A, Perini G, Lecchi M, Mariani C, Lucignani G, Clerici F. Correlation between 123I-FP-CIT brain SPECT and parkinsonism in dementia with Lewy bodies: caveat for clinical use. Clin Nucl Med. 2015; 40(01):32–35. DOI: 10.1097/RLU.0000000000000602 [PubMed: 25290294]

196. Walker Z, Jaros E, Walker RWH, et al. Dementia with Lewy bodies: a comparison of clinical diagnosis, FP-CIT single photon emission computed tomography imaging and autopsy. J Neurol Neurosurg Psychiatry. 2007; 78(11):1176–1181. DOI: 10.1136/jnnp.2006.110122 [PubMed: 17353255]

197. Papathanasiou ND, Boutsiadis A, Dickson J, Bomanji JB. Diagnostic accuracy of ^{123}I-FP-CIT (DaTSCAN) in dementia with Lewy bodies: a meta-analysis of published studies. Parkinsonism Relat Disord. 2012; 18(03):225–229. DOI: 10.1016/j.parkreldis.2011.09.015 [PubMed: 21975260]

198. Siepel FJ, Rongve A, Buter TC, et al. (123I)FP-CIT SPECT in suspected dementia with Lewy bodies: a longitudinal case study. BMJ Open. 2013; 3(04):e002642.doi: 10.1136/bmjopen-2013-002642

199. van der Zande JJ, Booij J, Scheltens P, Raijmakers PGHM, Lemstra AW. [(123)]FP-CIT SPECT scans initially rated as normal became abnormal over time in patients with probable dementia with Lewy bodies. Eur J Nucl Med Mol Imaging. 2016; 43(06):1060–1066. DOI: 10.1007/s00259-016-3312-x [PubMed: 26830298]

200. O'Brien JT, Colloby S, Fenwick J, et al. Dopamine transporter loss visualized with FP-CIT SPECT in the differential diagnosis of dementia with Lewy bodies. Arch Neurol. 2004; 61(06):919–925. DOI: 10.1001/archneur.61.6.919 [PubMed: 15210531]

201. Kantarci K, Lowe VJ, Boeve BF, et al. Multimodality imaging characteristics of dementia with Lewy bodies. Neurobiol Aging. 2012; 33(09):2091–2105. DOI: 10.1016/j.neurobiolaging.2011.09.024 [PubMed: 22018896]

202. Gilman S, Koeppe RA, Little R, et al. Differentiation of Alzheimer's disease from dementia with Lewy bodies utilizing positron emission tomography with [18F] fluorodeoxyglucose and neuropsychological testing. Exp Neurol. 2005; 191(Suppl 1):S95–S103. DOI: 10.1016/j.expneurol.2004.06.017 [PubMed: 15629765]

203. Pagano G, Niccolini F, Politis M. Imaging in Parkinson's disease. Clin Med (Lond). 2016; 16(04):371–375. doi:10.7861/clinmedi-cine.16-4-371(Northfield Il). [PubMed: 27481384]

204. Zhang X, Jin H, Padakanti PK, et al. Radiosynthesis and in Vivo Evaluation of Two PET Radioligands for Imaging α-Synuclein. Appl Sci (Basel). 2014; 4(01):66–78. DOI: 10.3390/app4010066 [PubMed: 25642331]

205. Geschwind MD. Rapidly Progressive Dementia. Continuum (Minneap Minn). 2016; 22(2 Dementia):510–537. [PubMed: 27042906]

206. Mead S, Rudge P. CJD mimics and chameleons. Pract Neurol. 2017; 17(02):113–121. [PubMed: 28153848]

207. Masters CL, Harris JO, Gajdusek DC, Gibbs CJ Jr, Bernoulli C, Asher DM. Creutzfeldt-Jakob disease: patterns of worldwide occurrence and the significance of familial and sporadic clustering. Ann Neurol. 1979; 5(02):177–188. DOI: 10.1002/ana.410050212 [PubMed: 371520]

208. Kovács GG, Puopolo M, Ladogana A, et al. EUROCJD. Genetic prion disease: the EUROCJD experience. Hum Genet. 2005; 118(02):166–174. DOI: 10.1007/s00439-005-0020-1 [PubMed: 16187142]

209. Ladogana A, Puopolo M, Poleggi A, et al. High incidence of genetic human transmissible spongiform encephalopathies in Italy. Neurology. 2005; 64(09):1592–1597. DOI: 10.1212/01.WNL.0000160118.26865.11 [PubMed: 15883322]

210. Takada LT, Kim M-O, Cleveland RW, et al. Genetic prion disease: experience of a rapidly progressive dementia center in the United States and a review of the literature. Am J Med Genet B Neuropsychiatr Genet. 2017; 174(01):36–69. DOI: 10.1002/ajmg.b.32505 [PubMed: 27943639]

211. Kretzschmar HA, Ironside JW, DeArmond SJ, Tateishi J. Diagnostic criteria for sporadic Creutzfeldt-Jakob disease. Arch Neurol. 1996; 53(09):913–920. [Accessed June 22, 2017] http://www.ncbi.nlm.nih.gov/pubmed/8815857. [PubMed: 8815857]

212. Geschwind MD. Prion Diseases. Continuum (Minneap Minn). 2015; 21(6 Neuroinfectious Disease):1612–1638. [PubMed: 26633779]

213. Wang LH, Bucelli RC, Patrick E, et al. Role of magnetic resonance imaging, cerebrospinal fluid, and electroencephalogram in diagnosis of sporadic Creutzfeldt-Jakob disease. J Neurol. 2013; 260(02):498–506. DOI: 10.1007/s00415-012-6664-6 [PubMed: 22968768]

214. Carswell C, Thompson A, Lukic A, et al. MRI findings are often missed in the diagnosis of Creutzfeldt-Jakob disease. BMC Neurol. 2012; 12(01):153.doi: 10.1186/1471-2377-12-153 [PubMed: 23216655]

215. Vitali P, MacCagnano E, Caverzasi E, Henry RG, Haman A, Torres-Chae C, et al. Diffusion-weighted MRI hyperintensity patterns differentiate CJD from other rapid dementias. Neurology. 2011; 76:1711–1719. [PubMed: 21471469]

216. Shiga Y, Miyazawa K, Sato S, et al. Diffusion-weighted MRI abnormalities as an early diagnostic marker for Creutzfeldt-Jakob disease. Neurology. 2004; 63(03):443–449. [Accessed June 22, 2017] http://www.ncbi.nlm.nih.gov/pubmed/15304574. [PubMed: 15304574]

217. Young GS, Geschwind MD, Fischbein NJ, et al. Diffusion-weighted and fluid-attenuated inversion recovery imaging in Creutzfeldt-Jakob disease: high sensitivity and specificity for diagnosis. AJNR Am J Neuroradiol. 2005; 26(06):1551–1562. [Accessed June 22, 2017] http://www.ncbi.nlm.nih.gov/pubmed/15956529. [PubMed: 15956529]

218. Puoti G, Bizzi A, Forloni G, Safar JG, Tagliavini F, Gambetti P. Sporadic human prion diseases: molecular insights and diagnosis. Lancet Neurol. 2012; 11(07):618–628. DOI: 10.1016/S1474-4422(12)70063-7 [PubMed: 22710755]

219. Bongianni M, Orrù C, Groveman BR, et al. Diagnosis of Human Prion Disease Using Real-Time Quaking-Induced Conversion Testing of Olfactory Mucosa and Cerebrospinal Fluid Samples. JAMA Neurol. 2017; 74(02):155–162. DOI: 10.1001/jamaneurol.2016.4614 [PubMed: 27942718]

220. Jezzard P, Barnett AS, Pierpaoli C. Characterization of and correction for eddy current artifacts in echo planar diffusion imaging. Magn Reson Med. 1998; 39(05):801–812. [Accessed June 22, 2017] http://www.ncbi.nlm.nih.gov/pubmed/9581612. [PubMed: 9581612]

221. Kong A, Kleinig T, Van der Vliet A, et al. MRI of sporadic Creutzfeldt-Jakob disease. J Med Imaging Radiat Oncol. 2008; 52(04):318–324. DOI: 10.1111/j.1440-1673.2008.01962.x [PubMed: 18811754]

222. Cali I, Castellani R, Yuan J, et al. Classification of sporadic Creutzfeldt-Jakob disease revisited. Brain. 2006; 129(Pt 9):2266–2277. DOI: 10.1093/brain/awl224 [PubMed: 16923954]

223. Meissner B, Kallenberg K, Sanchez-Juan P, et al. MRI lesion profiles in sporadic Creutzfeldt-Jakob disease. Neurology. 2009; 72(23):1994–2001. DOI: 10.1212/WNL.0b013e3181a96e5d [PubMed: 19506221]

224. Caverzasi E, Henry RG, Vitali P, et al. Application of quantitative DTI metrics in sporadic CJD. Neuroimage Clin. 2014; 4:426–435. DOI: 10.1016/j.nicl.2014.01.011 [PubMed: 24624328]

225. Caverzasi E, Mandelli ML, DeArmond SJ, et al. White matter involvement in sporadic Creutzfeldt-Jakob disease. Brain. 2014; 137(Pt 12):3339–3354. DOI: 10.1093/brain/awu298 [PubMed: 25367029]

226. Paoletti, M., Caverzasi, E., Mandelli, ML., et al. Sporadic Creutzfeld-Jacob Disease quantitative diffusion profiles and resting state functional correlates. ePoster Presented at International Society for Magnetic Resonance in Medicine Annual Meeting; 2017;

227. Rudge P, Jaunmuktane Z, Adlard P, et al. Iatrogenic CJD due to pituitary-derived growth hormone with genetically determined incubation times of up to 40 years. Brain. 2015; 138(Pt 11):3386–3399. DOI: 10.1093/brain/awv235 [PubMed: 26268531]

228. Lewis AM, Yu M, DeArmond SJ, Dillon WP, Miller BL, Geschwind MD. Human growth hormone-related iatrogenic Creutzfeldt-Jakob disease with abnormal imaging. Arch Neurol. 2006; 63(02):288–290. DOI: 10.1001/archneur.63.2.288 [PubMed: 16476821]

229. Macfarlane RG, Wroe SJ, Collinge J, Yousry TA, Jäger HR. Neuroimaging findings in human prion disease. J Neurol Neurosurg Psychiatry. 2007; 78(07):664–670. DOI: 10.1136/jnnp. 2006.094821 [PubMed: 17135459]

230. Zeidler M, Sellar RJ, Collie DA, et al. The pulvinar sign on magnetic resonance imaging in variant Creutzfeldt-Jakob disease. Lancet. 2000; 355(9213):1412–1418. DOI: 10.1016/s0140-6736(00)02140-1 [PubMed: 10791525]

231. Haïk S, Brandel JP, Oppenheim C, et al. Sporadic CJD clinically mimicking variant CJD with bilateral increased signal in the pulvinar. Neurology. 2002; 58(01):148–149. [Accessed June 22, 2017] http://www.ncbi.nlm.nih.gov/pubmed/11781427.

232. Martindale J, Geschwind MD, De Armond S, et al. Sporadic Creutzfeldt-Jakob disease mimicking variant Creutzfeldt-Jakob disease. Arch Neurol. 2003; 60(05):767–770. DOI: 10.1001/archneur. 60.5.767 [PubMed: 12756143]

233. Breithaupt M, Romero C, Kallenberg K, et al. Magnetic resonance imaging in E200K and V210I mutations of the prion protein gene. Alzheimer Dis Assoc Disord. 2013; 27(01):87–90. DOI: 10.1097/WAD.0b013e31824d578a [PubMed: 22407223]

234. Krasnianski A, Heinemann U, Ponto C, et al. Clinical findings and diagnosis in genetic prion diseases in Germany. Eur J Epidemiol. 2016; 31(02):187–196. DOI: 10.1007/s10654-015-0049-y [PubMed: 26076917]

235. Krasnianski A, Bartl M, Sanchez Juan PJ, et al. Fatal familial insomnia: clinical features and early identification. Ann Neurol. 2008; 63(05):658–661. DOI: 10.1002/ana.21358 [PubMed: 18360821]

236. Shi Q, Zhou W, Chen C, et al. The features of genetic prion diseases based on Chinese surveillance program. PLoS One. 2015; 10(10):e0139552.doi: 10.1371/journal.pone.0139552 [PubMed: 26488179]

237. Singhal AB, Newstein MC, Budzik R, et al. Diffusion-weighted magnetic resonance imaging abnormalities in Bartonella encephalopathy. J Neuroimaging. 2003; 13(01):79–82. DOI: 10.1177/1051228402239722 [PubMed: 12593136]

238. Sener RN. Pantothenate kinase-associated neurodegeneration: MR imaging, proton MR spectroscopy, and diffusion MR imaging findings. Am J Neuroradiol. 2003; 24:1690–1693. [PubMed: 13679293]

239. Halavaara J, Brander A, Lyytinen J, Setälä K, Kallela M. Wernicke's encephalopathy: is diffusion-weighted MRI useful? Neuroradiology. 2003; 45(08):519–523. DOI: 10.1007/s00234-003-1043-8 [PubMed: 12861431]

240. Weiss D, Brockmann K, Nägele T, Gasser T, Krüger R. Rapid emergence of temporal and pulvinar lesions in MELAS mimicking Creutzfeldt-Jakob disease. Neurology. 2011; 77(09):914.doi: 10.1212/WNL.0b013e31822c6275 [PubMed: 21876197]

241. Geschwind MD, Tan KM, Lennon VA, et al. Voltage-gated potassium channel autoimmunity mimicking Creutzfeldt-Jakob disease. Arch Neurol. 2008; 65(10):1341–1346. DOI: 10.1001/archneur.65.10.1341 [PubMed: 18852349]

242. Rosenbloom MH, Tartaglia MC, Forner SA, et al. Metabolic disorders with clinical and radiologic features of sporadic Creutzfeldt-Jakob disease. Neurol Clin Pract. 2015; 5(02):108–115. DOI: 10.1212/CPJ.0000000000000114 [PubMed: 26137419]

243. Chu K, Kang D-W, Kim J-Y, Chang K-H, Lee SK. Diffusion-weighted magnetic resonance imaging in nonconvulsive status epilepticus. Arch Neurol. 2001; 58(06):993–998. DOI: 10.1001/archneur.58.6.993 [PubMed: 11405815]

244. Flanagan, EP., Drubach, DA., Boeve, BF. Autoimmune Dementia and Encephalopathy. In: Pittok, SJ., Vincent, A., editors. Handbook of clinical neurology. Netherlands: Elsevier; 2016. p. 247-267.

245. Misra UK, Kalita J, Phadke RV, et al. Usefulness of various MRI sequences in the diagnosis of viral encephalitis. Acta Trop. 2010; 116(03):206–211. DOI: 10.1016/j.actatropica.2010.08.007 [PubMed: 20816658]

246. Fugate JE, Claassen DO, Cloft HJ, Kallmes DF, Kozak OS, Rabinstein AA. Posterior reversible encephalopathy syndrome: associated clinical and radiologic findings. Mayo Clin Proc. 2010; 85(05):427–432. DOI: 10.4065/mcp.2009.0590 [PubMed: 20435835]

247. Geschwind MD, Haman A, Miller BL. Rapidly progressive dementia. Neurol Clin. 2007; 25(03):783–807. vii. DOI: 10.1016/j.ncl.2007.04.001 [PubMed: 17659190]

248. Hakim S, Adams RD. The special clinical problem of symptomatic hydrocephalus with normal cerebrospinal fluid pressure. Observations on cerebrospinal fluid hydrodynamics. J Neurol Sci. 1965; 2(04):307–327. DOI: 10.1016/0022-510X(65)90016-X [PubMed: 5889177]

249. Relkin N, Marmarou A, Klinge P, Bergsneider M, Black PM. Diagnosing idiopathic normal-pressure hydrocephalus. Neurosurgery. 2005; 57(3, Suppl):S4–S16. discussion ii–v. [PubMed: 16160425]

250. Klinge P, Hellström P, Tans J, Wikkelsø C. European iNPH Multicentre Study Group. One-year outcome in the European multicentre study on iNPH. Acta Neurol Scand. 2012; 126(03):145–153. DOI: 10.1111/j.1600-0404.2012.01676.x [PubMed: 22571428]

251. Craven CL, Toma AK, Mostafa T, Patel N, Watkins LD. The predictive value of DESH for shunt responsiveness in idiopathic normal pressure hydrocephalus. J Clin Neurosci. 2016; 34:294–298. DOI: 10.1016/j.jocn.2016.09.004 [PubMed: 27692614]

252. Toma AK, Papadopoulos MC, Stapleton S, Kitchen ND, Watkins LD. Systematic review of the outcome of shunt surgery in idiopathic normal-pressure hydrocephalus. Acta Neurochir (Wien). 2013; 155(10):1977–1980. DOI: 10.1007/s00701-013-1835-5 [PubMed: 23975646]

253. Toma AK, Watkins LD. Surgical management of idiopathic normal pressure hydrocephalus: a trial of a trial. Br J Neurosurg. 2016; 30(06):605.doi: 10.1080/02688697.2016.1229751 [PubMed: 27626959]

254. Toma AK, Holl E, Kitchen ND, Watkins LD. Evans' index revisited: the need for an alternative in normal pressure hydrocephalus. Neurosurgery. 2011; 68(04):939–944. DOI: 10.1227/NEU.0b013e318208f5e0 [PubMed: 21221031]

255. Ambarki K, Israelsson H, Wåhlin A, Birgander R, Eklund A, Malm J. Brain ventricular size in healthy elderly: comparison between Evans index and volume measurement. Neurosurgery. 2010; 67(01):94–99. discussion 99. DOI: 10.1227/01.NEU.0000370939.30003.D1 [PubMed: 20559096]

256. García-Valdecasas-Campelo E, González-Reimers E, Santolaria-Fernández F, et al. Brain atrophy in alcoholics: relationship with alcohol intake; liver disease; nutritional status, and inflammation. Alcohol Alcohol. 2007; 42(06):533–538. DOI: 10.1093/alcalc/agm065 [PubMed: 17855333]

257. Brunberg JA, Jacquemont S, Hagerman RJ, et al. Fragile X pre-mutation carriers: characteristic MR imaging findings of adult male patients with progressive cerebellar and cognitive dysfunction. AJNR Am J Neuroradiol. 2002; 23(10):1757–1766. [PubMed: 12427636]

258. Ishii K, Soma T, Shimada K, Oda H, Terashima A, Kawasaki R. Automatic volumetry of the cerebrospinal fluid space in idiopathic normal pressure hydrocephalus. Dement Geriatr Cogn Dis Extra. 2013; 3(01):489–496. DOI: 10.1159/000357329 [PubMed: 24516417]

259. Hashimoto M, Ishikawa M, Mori E, Kuwana N. Study of INPH on neurological improvement (SINPHONI). Diagnosis of idiopathic normal pressure hydrocephalus is supported by MRI-based scheme: a prospective cohort study. Cerebrospinal Fluid Res. 2010; 7(01):18.doi: 10.1186/1743-8454-7-18 [PubMed: 21040519]

260. Krauss JK, Regel JP, Vach W, Jüngling FD, Droste DW, Wakhloo AK. Flow void of cerebrospinal fluid in idiopathic normal pressure hydrocephalus of the elderly: can it predict outcome after shunting? Neurosurgery. 1997; 40(01):67–73. discussion 73–74. [PubMed: 8971826]

261. Bradley WG Jr. CSF Flow in the Brain in the Context of Normal Pressure Hydrocephalus. AJNR Am J Neuroradiol. 2015; 36(05):831–838. DOI: 10.3174/ajnr.A4124 [PubMed: 25355813]

262. Virhammar J, Laurell K, Cesarini KG, Larsson EM. Preoperative prognostic value of MRI findings in 108 patients with idiopathic normal pressure hydrocephalus. AJNR Am J Neuroradiol. 2014; 35(12):2311–2318. [PubMed: 25012669]

263. Del Bigio MR. Neuropathological changes caused by hydrocephalus. Acta Neuropathol. 1993; 85(06):573–585. DOI: 10.1007/BF00334666 [PubMed: 8337936]

264. Tullberg M, Hultin L, Ekholm S, Månsson J-E, Fredman P, Wikkelsø C. White matter changes in normal pressure hydrocephalus and Binswanger disease: specificity, predictive value and correlations to axonal degeneration and demyelination. Acta Neurol Scand. 2002; 105(06):417–426. [PubMed: 12027829]

265. Marumoto K, Koyama T, Hosomi M, Kodama N, Miyake H, Domen K. Diffusion tensor imaging in elderly patients with idiopathic normal pressure hydrocephalus or Parkinson's disease: diagnosis of gait abnormalities. Fluids Barriers CNS. 2012; 9(01):20.doi: 10.1186/2045-8118-9-20 [PubMed: 22989298]

266. Ho ínek D, Štěpán-Buksakowska I, Szabó N, et al. Difference in white matter microstructure in differential diagnosis of normal pressure hydrocephalus and Alzheimer's disease. Clin Neurol Neurosurg. 2016; 140:52–59. DOI: 10.1016/j.clineuro.2015.11.010 [PubMed: 26646649]

267. Hoza D, Vlasák A, Ho ínek D, Sameš M, Alfieri A. DTI-MRI biomarkers in the search for normal pressure hydrocephalus aetiology: a review. Neurosurg Rev. 2015; 38(02):239–244. discussion 244. DOI: 10.1007/s10143-014-0584-0 [PubMed: 25345377]

268. Siasios I, Kapsalaki EZ, Fountas KN, et al. The role of diffusion tensor imaging and fractional anisotropy in the evaluation of patients with idiopathic normal pressure hydrocephalus: a literature review. Neurosurg Focus. 2016; 41(03):E12.doi: 10.3171/2016.6.FOCUS16192

269. Kim MJ, Seo SW, Lee KM, et al. Differential diagnosis of idiopathic normal pressure hydrocephalus from other dementias using diffusion tensor imaging. AJNR Am J Neuroradiol. 2011; 32(08):1496–1503. DOI: 10.3174/ajnr.A2531 [PubMed: 21700790]

270. Yamada S, Tsuchiya K, Bradley WG, et al. Current and emerging MR imaging techniques for the diagnosis and management of CSF fkow disorders: a review of phase-contrast and time-spatial labeling inversion pulse. AJNR Am J Neuroradiol. 2015; 36(04):623–630. DOI: 10.3174/ajnr.A4030 [PubMed: 25012672]

271. Khoo HM, Kishima H, Tani N, et al. Default mode network connectivity in patients with idiopathic normal pressure hydrocephalus. J Neurosurg. 2016; 124(02):350–358. DOI: 10.3171/2015.1.JNS141633 [PubMed: 26295919]

272. Gilman S, Wenning GK, Low PA, et al. Second consensus statement on the diagnosis of multiple system atrophy. Neurology. 2008; 71(09):670–676. [PubMed: 18725592]

273. Joutsa J, Gardberg M, Röyttä M, Kaasinen V. Diagnostic accuracy of parkinsonism syndromes by general neurologists. Parkinsonism Relat Disord. 2014; 20(08):840–844. DOI: 10.1016/j.parkreldis.2014.04.019 [PubMed: 24816002]

274. Hughes AJ, Daniel SE, Ben-Shlomo Y, Lees AJ. The accuracy of diagnosis of parkinsonian syndromes in a specialist movement disorder service. Brain. 2002; 125(Pt 4):861–870. [Accessed June 6, 2017] http://www.ncbi.nlm.nih.gov/pubmed/11912118. [PubMed: 11912118]

275. Bürk K, Skalej M, Dichgans J. Pontine MRI hyperintensities ("the cross sign") are not pathognomonic for multiple system atrophy (MSA). Mov Disord. 2001; 16(03):535.doi: 10.1002/mds.1107 [PubMed: 11391754]

276. Abe K, Hikita T, Yokoe M, Mihara M, Sakoda S. The "cross" signs in patients with multiple system atrophy: a quantitative study. J Neuroimaging. 2006; 16(01):73–77. DOI: 10.1177/1051228405279988 [PubMed: 16483280]

277. Kasahara S, Miki Y, Kanagaki M, et al. "Hot cross bun" sign in multiple system atrophy with predominant cerebellar ataxia: a comparison between proton density-weighted imaging and T2-weighted imaging. Eur J Radiol. 2012; 81(10):2848–2852. DOI: 10.1016/j.ejrad.2011.12.012 [PubMed: 22209432]

278. Schrag A, Good CD, Miszkiel K, et al. Differentiation of atypical parkinsonian syndromes with routine MRI. Neurology. 2000; 54(03):697–702. DOI: 10.1212/WNL.55.8.1239-a [PubMed: 10680806]

279. Horimoto Y, Aiba I, Yasuda T, et al. Longitudinal MRI study of multiple system atrophy - when do the findings appear, and what is the course? J Neurol. 2002; 249(07):847–854. DOI: 10.1007/s00415-002-0734-0 [PubMed: 12140668]

280. Takao M, Kadowaki T, Tomita Y, Yoshida Y, Mihara B. 'Hot-cross bun sign' of multiple system atrophy. Intern Med. 2007; 46(22):1883.doi: 10.2169/internalmedicine.46.0514 [PubMed: 18025774]

281. Mandelli ML, De Simone T, Minati L, et al. Diffusion tensor imaging of spinocerebellar ataxias types 1 and 2. AJNR Am J Neuroradiol. 2007; 28(10):1996–2000. DOI: 10.3174/ajnr.A0716 [PubMed: 17998418]

282. Loy CT, Sweeney MG, Davis MB, et al. Spinocerebellar ataxia type 17: extension of phenotype with putaminal rim hyperintensity on magnetic resonance imaging. Mov Disord. 2005; 20(11):1521–1523. DOI: 10.1002/mds.20529 [PubMed: 16037935]

283. Schöls L, Bauer P, Schmidt T, Schulte T, Riess O. Autosomal dominant cerebellar ataxias: clinical features, genetics, and pathogenesis. Lancet Neurol. 2004; 3(05):291–304. DOI: 10.1016/S1474-4422(04)00737-9 [PubMed: 15099544]

284. Soares-Fernandes JP, Ribeiro M, Machado A. "Hot cross bun" sign in variant Creutzfeldt-Jakob disease. AJNR Am J Neuroradiol. 2009; 30(03):E37.doi: 10.3174/ajnr.A1335 [PubMed: 19279286]

285. Muqit MM, Mort D, Miskiel KA, Shakir RA. "Hot cross bun" sign in a patient with parkinsonism secondary to presumed vasculitis. J Neurol Neurosurg Psychiatry. 2001; 71(04):565–566. [PubMed: 11601421]

286. Tha KK, Terae S, Tsukahara A, et al. Hyperintense putaminal rim at 1. 5 T: prevalence in normal subjects and distinguishing features from multiple system atrophy. BMC Neurol. 2012; 12(01):39.doi: 10.1186/1471-2377-12-39 [PubMed: 22708511]

287. Ghaemi M, Hilker R, Rudolf J, Sobesky J, Heiss WD. Differentiating multiple system atrophy from Parkinson's disease: contribution of striatal and midbrain MRI volumetry and multi-tracer PET imaging. J Neurol Neurosurg Psychiatry. 2002; 73(05):517–523. DOI: 10.1136/jnnp.73.5.517 [PubMed: 12397143]

288. Brenneis C, Seppi K, Schocke MF, et al. Voxel-based morphometry detects cortical atrophy in the Parkinson variant of multiple system atrophy. Mov Disord. 2003; 18(10):1132–1138. DOI: 10.1002/mds.10502 [PubMed: 14534916]

289. Specht K, Minnerop M, Abele M, Reul J, Wüllner U, Klockgether T. In vivo voxel-based morphometry in multiple system atrophy of the cerebellar type. Arch Neurol. 2003; 60(10):1431–1435. DOI: 10.1001/archneur.60.10.1431 [PubMed: 14568814]

290. Brenneis C, Boesch SM, Egger KE, et al. Cortical atrophy in the cerebellar variant of multiple system atrophy: a voxel-based morphometry study. Mov Disord. 2006; 21(02):159–165. DOI: 10.1002/mds.20656 [PubMed: 16161039]

291. Minnerop M, Specht K, Ruhlmann J, et al. Voxel-based morphometry and voxel-based relaxometry in multiple system atrophy-a comparison between clinical subtypes and correlations with clinical parameters. Neuroimage. 2007; 36(04):1086–1095. DOI: 10.1016/j.neuroimage.2007.04.028 [PubMed: 17512219]

292. Brenneis C, Egger K, Scherfler C, et al. Progression of brain atrophy in multiple system atrophy. A longitudinal VBM study. J Neurol. 2007; 254(02):191–196. DOI: 10.1007/s00415-006-0325-6 [PubMed: 17334661]

293. Schulz JB, Skalej M, Wedekind D, et al. Magnetic resonance imaging-based volumetry differentiates idiopathic Parkinson's syndrome from multiple system atrophy and progressive supranuclear palsy. Ann Neurol. 1999; 45(01):65–74. [Accessed June 22, 2017] http://www.ncbi.nlm.nih.gov/pubmed/9894879. [PubMed: 9894879]

294. Ngai S, Tang YM, Du L, Stuckey S. Hyperintensity of the middle cerebellar peduncles on fluid-attenuated inversion recovery imaging: variation with age and implications for the diagnosis of multiple system atrophy. AJNR Am J Neuroradiol. 2006; 27(10):2146–2148. [PubMed: 17110685]

295. Lee EA, Cho HI, Kim SS, Lee WY. Comparison of magnetic resonance imaging in subtypes of multiple system atrophy. Parkinsonism Relat Disord. 2004; 10(06):363–368. DOI: 10.1016/j.parkreldis.2004.04.008 [PubMed: 15261878]

296. Bhattacharya K, Saadia D, Eisenkraft B, et al. Brain magnetic resonance imaging in multiple-system atrophy and Parkinson disease: a diagnostic algorithm. Arch Neurol. 2002; 59(05):835–842. [PubMed: 12020268]

297. Worker A, Blain C, Jarosz J, et al. Diffusion tensor imaging of Parkinson's disease, multiple system atrophy and progressive supranuclear palsy: a tract-based spatial statistics study. PLoS One. 2014; 9(11):e112638.doi: 10.1371/journal.pone.0112638 [PubMed: 25405990]

298. Schocke MFH, Seppi K, Esterhammer R, et al. Diffusion-weighted MRI differentiates the Parkinson variant of multiple system atrophy from PD. Neurology. 2002; 58(04):575–580. DOI: 10.1212/WNL.58.4.575 [PubMed: 11865135]

299. Schocke MFH, Seppi K, Esterhammer R, et al. Trace of diffusion tensor differentiates the Parkinson variant of multiple system atrophy and Parkinson's disease. Neuroimage. 2004; 21(04):1443–1451. DOI: 10.1016/j.neuroimage.2003.12.005 [PubMed: 15050569]

300. Seppi K, Schocke MFH, Prennschuetz-Schuetzenau K, et al. Topography of putaminal degeneration in multiple system atrophy: a diffusion magnetic resonance study. Mov Disord. 2006; 21(06):847–852. DOI: 10.1002/mds.20843 [PubMed: 16538620]

301. Nicoletti G, Lodi R, Condino F, et al. Apparent diffusion coefficient measurements of the middle cerebellar peduncle differentiate the Parkinson variant of MSA from Parkinson's disease and progressive supranuclear palsy. Brain. 2006; 129(Pt 10):2679–2687. DOI: 10.1093/brain/awl166 [PubMed: 16815875]

302. Paviour DC, Thornton JS, Lees AJ, Jäger HR. Diffusion-weighted magnetic resonance imaging differentiates Parkinsonian variant of multiple-system atrophy from progressive supranuclear palsy. Mov Disord. 2007; 22(01):68–74. DOI: 10.1002/mds.21204 [PubMed: 17089396]

303. Baudrexel S, Seifried C, Penndorf B, et al. The value of putaminal diffusion imaging versus 18-fluorodeoxyglucose positron emission tomography for the differential diagnosis of the Parkinson variant of multiple system atrophy. Mov Disord. 2014; 29(03):380–387. DOI: 10.1002/mds.25749 [PubMed: 24243813]

304. Kanazawa M, Shimohata T, Terajima K, et al. Quantitative evaluation of brainstem involvement in multiple system atrophy by diffusion-weighted MR imaging. J Neurol. 2004; 251(09):1121–1124. DOI: 10.1007/s00415-004-0494-0 [PubMed: 15372256]

305. Fulham MJ, Dubinsky RM, Polinsky RJ, et al. Computed tomography, magnetic resonance imaging and positron emission tomography with [18F]fluorodeoxyglucose in multiple system atrophy and pure autonomic failure. Clin Auton Res. 1991; 1(01):27–36. [Accessed June 6, 2017] http://www.ncbi.nlm.nih.gov/pubmed/1821662. [PubMed: 1821662]

306. Bosman T, Van Laere K, Santens P. Anatomically standardised 99mTc-ECD brain perfusion SPET allows accurate differentiation between healthy volunteers, multiple system atrophy and idiopathic Parkinson's disease. Eur J Nucl Med Mol Imaging. 2003; 30(01):16–24. DOI: 10.1007/s00259-002-1009-9 [PubMed: 12483405]

307. Cilia R, Marotta G, Benti R, Pezzoli G, Antonini A. Brain SPECT imaging in multiple system atrophy. J Neural Transm (Vienna). 2005; 112(12):1635–1645. DOI: 10.1007/s00702-005-0382-5 [PubMed: 16284908]

308. Kim YJ, Ichise M, Ballinger JR, et al. Combination of dopamine transporter and D2 receptor SPECT in the diagnostic evaluation of PD, MSA, and PSP. Mov Disord. 2002; 17(02):303–312. [Accessed June 6, 2017] http://www.ncbi.nlm.nih.gov/pubmed/11921116. [PubMed: 11921116]

309. Perlman, S. Evaluation and Management of Ataxic Disorders: An Overview for Physicians. Minneapolis, MN: National Ataxia Foundation; 2007.

310. Klockgether T, Skalej M, Wedekind D, et al. Autosomal dominant cerebellar ataxia type I. MRI-based volumetry of posterior fossa structures and basal ganglia in spinocerebellar ataxia types 1, 2 and 3. Brain. 1998; 121(Pt 9):1687–1693. [PubMed: 9762957]

311. Brenneis C, Bösch SM, Schocke M, Wenning GK, Poewe W. Atrophy pattern in SCA2 determined by voxel-based morphometry. Neuroreport. 2003; 14(14):1799–1802. DOI: 10.1097/00001756-200310060-00008 [PubMed: 14534423]

312. Lin IS, Wu RM, Lee-Chen GJ, Shan DE, Gwinn-Hardy K. The SCA17 phenotype can include features of MSA-C, PSP and cognitive impairment. Parkinsonism Relat Disord. 2007; 13(04): 246–249. DOI: 10.1016/j.parkreldis.2006.04.009 [PubMed: 16793320]

313. Schöls L, Amoiridis G, Epplen JT, Langkafel M, Przuntek H, Riess O. Relations between genotype and phenotype in German patients with the Machado-Joseph disease mutation. J Neurol Neurosurg Psychiatry. 1996; 61(05):466–470. DOI: 10.1136/jnnp.61.5.466 [PubMed: 8937340]

314. Schöls L, Haan J, Riess O, Amoiridis G, Przuntek H. Sleep disturbance in spinocerebellar ataxias: is the SCA3 mutation a cause of restless legs syndrome? Neurology. 1998; 51(06):1603–1607. [PubMed: 9855509]

315. Lima L, Coutinho P. Clinical criteria for diagnosis of Machado-Joseph disease: report of a non-Azorena Portuguese family. Neurology. 1980; 30(03):319–322. [Accessed June 6, 2017] http://www.ncbi.nlm.nih.gov/pubmed/7189034. [PubMed: 7189034]

316. Murata Y, Yamaguchi S, Kawakami H, et al. Characteristic magnetic resonance imaging findings in Machado-Joseph disease. Arch Neurol. 1998; 55(01):33–37. DOI: 10.1001/archneur.55.1.33 [PubMed: 9443709]

317. Harding AE. The clinical features and classification of the late onset autosomal dominant cerebellar ataxias. A study of 11 families, including descendants of the 'the Drew family of Walworth'. Brain. 1982; 105(Pt 1):1–28. [Accessed June 6, 2017] http://www.ncbi.nlm.nih.gov/pubmed/7066668. [PubMed: 7066668]

318. Harding AE. "Idiopathic" late onset cerebellar ataxia". A clinical and genetic study of 36 cases. J Neurol Sci. 1981; 51(02):259–271. [PubMed: 7276977]

319. Kerber KA, Jen JC, Perlman S, Baloh RW. Late-onset pure cerebellar ataxia: differentiating those with and without identifiable mutations. J Neurol Sci. 2005; 238(1–2):41–45. DOI: 10.1016/j.jns.2005.06.006 [PubMed: 16109427]

320. Wardle M, Majounie E, Muzaimi MB, Williams NM, Morris HR, Robertson NP. The genetic aetiology of late-onset chronic progressive cerebellar ataxia. A population-based study. J Neurol. 2009; 256(03):343–348. DOI: 10.1007/s00415-009-0015-2 [PubMed: 19259763]

321. Brussino A, Gellera C, Saluto A, et al. FMR1 gene premutation is a frequent genetic cause of late-onset sporadic cerebellar ataxia. Neurology. 2005; 64(01):145–147. DOI: 10.1212/01.WNL.0000148723.37489.3F [PubMed: 15642922]

322. Bürk K, Bühring U, Schulz JB, Zühlke C, Hellenbroich Y, Dichgans J. Clinical and magnetic resonance imaging characteristics of sporadic cerebellar ataxia. Arch Neurol. 2005; 62(06):981–985. DOI: 10.1001/archneur.62.6.981 [PubMed: 15956170]

323. Koide R, Onodera O, Ikeuchi T, et al. Atrophy of the cerebellum and brainstem in dentatorubral pallidoluysian atrophy. Influence of CAG repeat size on MRI findings. Neurology. 1997; 49(06):1605–1612. DOI: 10.1212/WNL.49.6.1605 [PubMed: 9409354]

324. Jacquemont S, Hagerman RJ, Leehey M, et al. Fragile X premutation tremor/ataxia syndrome: molecular, clinical, and neuroimaging correlates. Am J Hum Genet. 2003; 72(04):869–878. DOI: 10.1086/374321 [PubMed: 12638084]

325. Jacquemont S, Farzin F, Hall D, et al. Aging in individuals with the FMR1 mutation. Am J Ment Retard. 2004; 109(02):154–164. DOI: 10.1352/0895-8017(2004)109<154:AIIWTF>2.0.CO;2 [PubMed: 15000674]

326. Chang CC, Eggers SD, Johnson JK, Haman A, Miller BL, Geschwind MD. Anti-GAD antibody cerebellar ataxia mimicking Creutzfeldt-Jakob disease. Clin Neurol Neurosurg. 2007; 109(01): 54–57. DOI: 10.1016/j.clineuro.2006.01.009 [PubMed: 16621241]

327. Peterson K, Rosenblum MK, Kotanides H, Posner JB. Paraneoplastic cerebellar degeneration. I. A clinical analysis of 55 anti-Yo antibody-positive patients. Neurology. 1992; 42(10):1931–1937. [Accessed June 6, 2017] http://www.ncbi.nlm.nih.gov/pubmed/1407575. [PubMed: 1407575]

328. Aylward EHH, Li Q, Stine OC, et al. Longitudinal change in basal ganglia volume in patients with Huntington's disease. Neurology. 1997; 48(02):394–399. DOI: 10.1212/WNL.48.2.394 [PubMed: 9040728]

329. Aylward EH, Nopoulos PC, Ross CA, et al. PREDICT-HD Investigators and Coordinators of Huntington Study Group. Longitudinal change in regional brain volumes in prodromal Huntington disease. J Neurol Neurosurg Psychiatry. 2011; 82(04):405–410. DOI: 10.1136/jnnp. 2010.208264 [PubMed: 20884680]

330. Ruocco HH, Bonilha L, Li LM, Lopes-Cendes I, Cendes F. Longitudinal analysis of regional grey matter loss in Huntington disease: effects of the length of the expanded CAG repeat. J Neurol Neurosurg Psychiatry. 2008; 79(02):130–135. DOI: 10.1136/jnnp.2007.116244 [PubMed: 17615168]

331. Apple AC, Possin KL, Satris G, et al. Quantitative 7T Phase Imaging in Premanifest Huntington Disease. Am J Neuroradiol. 2014; 35:1707–1713. [PubMed: 24742810]

332. Kim H, Kim JH, Possin KL, et al. Surface-based morphometry reveals caudate subnuclear structural damage in patients with premotor Huntington disease. Brain Imaging Behav. 2017; 11(05):1365–1372. DOI: 10.1007/s11682-016-9616-4 [PubMed: 27730480]

333. Vonsattel JP, Myers RH, Stevens TJ, Ferrante RJ, Bird ED, Richard-son EP Jr. Neuropathological classification of Huntington's disease. J Neuropathol Exp Neurol. 1985; 44(06):559–577. [Accessed June 6, 2017] http://www.ncbi.nlm.nih.gov/pubmed/2932539. [PubMed: 2932539]

334. Rosas HD, Koroshetz WJ, Chen YI, et al. Evidence for more widespread cerebral pathology in early HD: an MRI-based morphometric analysis. Neurology. 2003; 60(10):1615–1620. DOI: 10.1212/WNL.62.3.523-a [PubMed: 12771251]

335. Tabrizi SJ, Langbehn DR, Leavitt BR, et al. TRACK-HD investigators. Biological and clinical manifestations of Huntington's disease in the longitudinal TRACK-HD study: cross-sectional analysis of baseline data. Lancet Neurol. 2009; 8(09):791–801. DOI: 10.1016/S1474-4422(09)70170-X.Biological [PubMed: 19646924]

336. Ciarmiello A, Cannella M, Lastoria S, et al. Brain white-matter volume loss and glucose hypometabolism precede the clinical symptoms of Huntington's disease. J Nucl Med. 2006; 47(02):215–222. [PubMed: 16455626]

337. Paulsen JS, Magnotta VA, Mikos AE, et al. Brain structure in preclinical Huntington's disease. Biol Psychiatry. 2006; 59(01):57–63. DOI: 10.1016/j.biopsych.2005.06.003 [PubMed: 16112655]

338. Paulsen JS, Nopoulos PC, Aylward E, et al. PREDICT-HD Investigators and Coordinators of the Huntington's Study Group (HSG). Striatal and white matter predictors of estimated diagnosis for Huntington disease. Brain Res Bull. 2010; 82(3–4):201–207. DOI: 10.1016/j.brainresbull. 2010.04.003 [PubMed: 20385209]

339. Stoffers D, Sheldon S, Kuperman JM, Goldstein J, Corey-Bloom J, Aron AR. Contrasting gray and white matter changes in pre-clinical Huntington disease: an MRI study. Neurology. 2010; 74(15):1208–1216. DOI: 10.1212/WNL.0b013e3181d8c20a [PubMed: 20385893]

340. Rosas HD, Tuch DS, Hevelone ND, et al. Diffusion tensor imaging in presymptomatic and early Huntington's disease: selective white matter pathology and its relationship to clinical measures. Mov Disord. 2006; 21(09):1317–1325. DOI: 10.1002/mds.20979 [PubMed: 16755582]

341. Della Nave R, Ginestroni A, Tessa C, et al. Regional distribution and clinical correlates of white matter structural damage in Huntington disease: a tract-based spatial statistics study. AJNR Am J Neuroradiol. 2010; 31(09):1675–1681. DOI: 10.3174/ajnr.A2128 [PubMed: 20488902]

342. Bohanna I, Georgiou-Karistianis N, Sritharan A, et al. Diffusion tensor imaging in Huntington's disease reveals distinct patterns of white matter degeneration associated with motor and cognitive deficits. Brain Imaging Behav. 2011; 5(03):171–180. DOI: 10.1007/s11682-011-9121-8 [PubMed: 21437574]

343. Delmaire C, Dumas EM, Sharman MA, et al. The structural correlates of functional deficits in early huntington's disease. Hum Brain Mapp. 2013; 34(09):2141–2153. DOI: 10.1002/hbm. 22055 [PubMed: 22438242]

344. Paulsen JS, Zimbelman JL, Hinton SC, et al. fMRI biomarker of early neuronal dysfunction in presymptomatic Huntington's Disease. AJNR Am J Neuroradiol. 2004; 25(10):1715–1721. [PubMed: 15569736]

345. Reading SAJ, Dziorny AC, Peroutka LA, et al. Functional brain changes in presymptomatic Huntington's disease. Ann Neurol. 2004; 55(06):879–883. DOI: 10.1002/ana.20121 [PubMed: 15174024]

346. Paulsen JS. Functional imaging in Huntington's disease. Exp Neurol. 2009; 216(02):272–277. [PubMed: 19171138]

347. van den Bogaard SJA, Dumas EM, Milles J, et al. Magnetization transfer imaging in premanifest and manifest Huntington disease. AJNR Am J Neuroradiol. 2012; 33(05):884–889. [PubMed: 22241387]

348. Feigin A, Leenders KL, Moeller JR, et al. Metabolic network abnormalities in early Huntington's disease: an [(18)F]FDG PET study. J Nucl Med. 2001; 42(11):1591–1595. [Accessed June 22, 2017] http://www.ncbi.nlm.nih.gov/pubmed/11696626. [PubMed: 11696626]

349. Saft C, Schüttke A, Beste C, Andrich J, Heindel W, Pfleiderer B. fMRI reveals altered auditory processing in manifest and pre-manifest Huntington's disease. Neuropsychologia. 2008; 46(05): 1279–1289. DOI: 10.1016/j.neuropsychologia.2007.12.002 [PubMed: 18221758]

350. Novak MJU, Warren JD, Henley SMD, Draganski B, Frackowiak RS, Tabrizi SJ. Altered brain mechanisms of emotion processing in pre-manifest Huntington's disease. Brain. 2012; 135(Pt 4): 1165–1179. DOI: 10.1093/brain/aws024 [PubMed: 22505631]

351. Sturrock A, Laule C, Decolongon J, et al. Magnetic resonance spectroscopy biomarkers in premanifest and early Huntington disease. Neurology. 2010; 75(19):1702–1710. DOI: 10.1212/WNL.0b013e3181fc27e4 [PubMed: 21060093]

352. Binney RJ, Pankov A, Marx G, et al. Data-driven regions of interest for longitudinal change in three variants of frontotemporal lobar degeneration. Brain Behav. 2017; 7(04):e00675.doi: 10.1002/brb3.675 [PubMed: 28413716]

353. Pankov A, Binney RJ, Staffaroni AM, et al. Data-driven regions of interest for longitudinal change in frontotemporal lobar degeneration. Neuroimage Clin. 2015; 12:332–340. DOI: 10.1016/j.nicl.2015.08.002 [PubMed: 27547726]

354. Dupont A-C, Largeau B, Santiago Ribeiro MJ, Guilloteau D, Tronel C, Arlicot N. Translocator Protein-18 kDa (TSPO) Positron Emission Tomography (PET) Imaging and Its Clinical Impact in Neurodegenerative Diseases. Int J Mol Sci. 2017; 18(04):785.doi: 10.3390/ijms18040785

355. Bullmore ET, Bassett DS. Brain graphs: graphical models of the human brain connectome. Annu Rev Clin Psychol. 2011; 7(01):113–140. DOI: 10.1146/annurev-clinpsy-040510-143934 [PubMed: 21128784]

356. Rosazza C, Minati L. Resting-state brain networks: literature review and clinical applications. Neurol Sci. 2011; 32(05):773–785. DOI: 10.1007/s10072-011-0636-y [PubMed: 21667095]

357. Jones DT, Knopman DS, Gunter JL, et al. Alzheimer's Disease Neuroimaging Initiative. Cascading network failure across the Alzheimer's disease spectrum. Brain. 2016; 139(Pt 2):547–562. DOI: 10.1093/brain/awv338 [PubMed: 26586695]

358. Ranasinghe KG, Rankin KP, Pressman PS, et al. Distinct subtypes of behavioral-variant frontotemporal dementia based on patterns of network degeneration. JAMA Neurol. 2016; 73(09):1078–1088. DOI: 10.1001/jamaneurol.2016.2016 [PubMed: 27429218]

359. Griffa A, Baumann PS, Thiran J-P, Hagmann P. Structural connectomics in brain diseases. Neuroimage. 2013; 80:515–526. DOI: 10.1016/j.neuroimage.2013.04.056 [PubMed: 23623973]

360. Sawlani V. Diffusion-weighted imaging and apparent diffusion coefficient evaluation of herpes simplex encephalitis and Japanese encephalitis. J Neurol Sci. 2009; 287(1–2):221–226. DOI: 10.1016/j.jns.2009.07.010 [PubMed: 19732907]

361. Küker W, Nägele T, Schmidt F, Heckl S, Herrlinger U. Diffusion-weighted MRI in herpes simplex encephalitis: a report of three cases. Neuroradiology. 2004; 46(02):122–125. DOI: 10.1007/s00234-003-1145-3 [PubMed: 14747879]

362. Hufnagel A, Weber J, Marks S, et al. Brain diffusion after single seizures. Epilepsia. 2003; 44(01):54–63. [Accessed July 20, 2017] http://www.ncbi.nlm.nih.gov/pubmed/12581230. [PubMed: 12581230]

363. Milligan TA, Zamani A, Bromfield E. Frequency and patterns of MRI abnormalities due to status epilepticus. Seizure. 2009; 18(02):104–108. DOI: 10.1016/j.seizure.2008.07.004 [PubMed: 18723376]

364. Burdette JH, Elster AD, Ricci PE. Acute cerebral infarction: quantification of spin-density and T2 shine-through phenomena on diffusion-weighted MR images. Radiology. 1999; 212(02):333–339. DOI: 10.1148/radiology.212.2.r99au36333 [PubMed: 10429687]
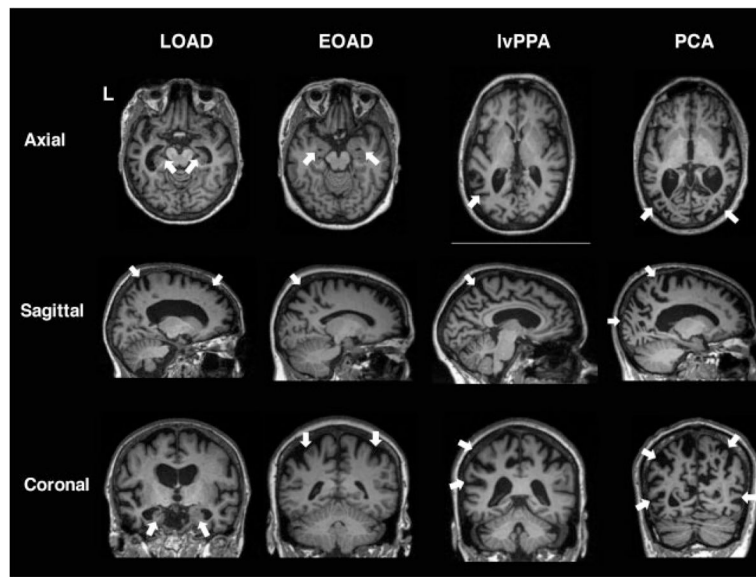
Fig. 1. T1 imaging in amyloid-PET confirmed AD variants

(**A**) LOAD 75-year-old female (MMSE: 17) with hippocampal atrophy on axial and coronal planes. Precuneus atrophy can be appreciated on sagittal imaging, along with some mild frontal atrophy. (**B**) EOAD 59-year-old female with cognitive impairments in multiple domains including memory and executive functioning (MMSE: 23; MOCA: 15). Prominent biparietal atrophy can be observed on sagittal and coronal planes, with relatively preserved medial temporal lobes on axial reconstruction compared with LOAD. (**C**) lvPPA female with lvPPA (MMSE: 28). Atrophy is lateralized to the left, primarily in the left temporoparietal region as seen on axial and coronal images. The precuneal atrophy observed on the sagittal images is typical of AD pathology. (**D**) PCA patient (MMSE: 18) with significant occipital and parietal atrophy, shown by arrows on all three planes. *Nonneurologic orientation (right is right). *Abbreviations: MMSE, mini-mental state examination; MoCA, Montreal Cognitive Assessment; LOAD, late onset Alzheimer's disease; EOAD, early onset Alzheimer's disease; PCA, posterior cortical atrophy.
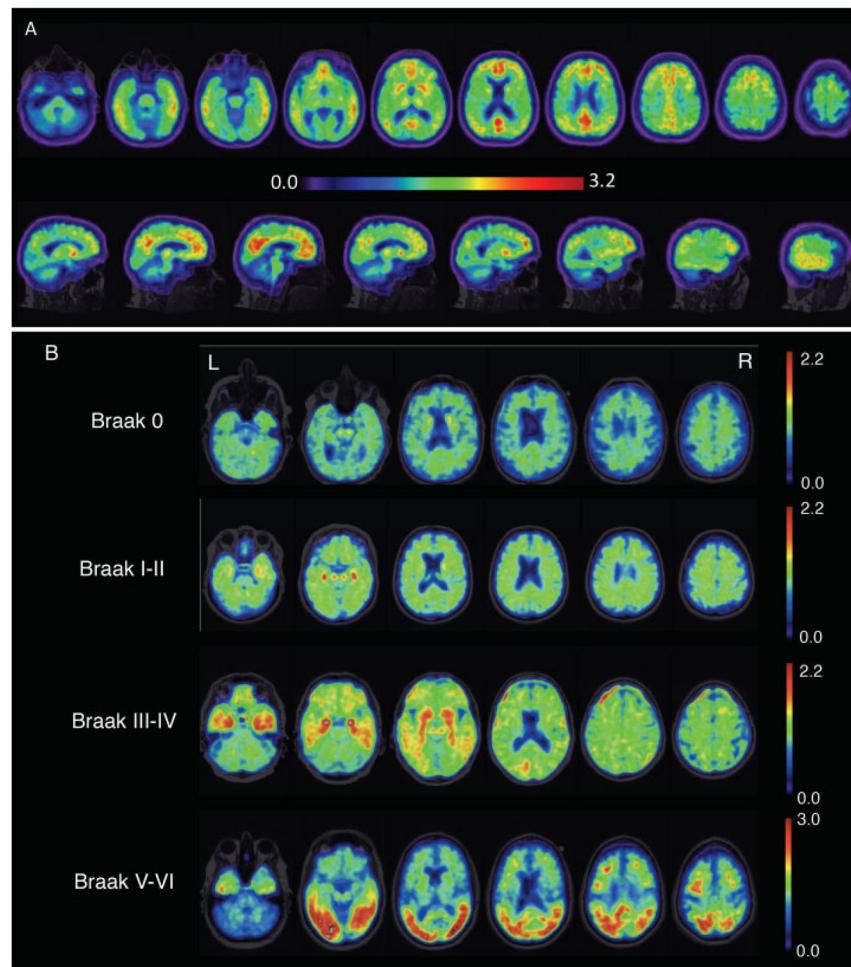
Fig. 2. Molecular positron emission tomography (PET) in Alzheimer's disease (AD)
(**A**) Amyloid PET using Pittsburgh compound B. Heat map range (colored bar) of amyloid tracer uptake defined by distribution volume ratio (DVR). Amyloid PET has been approved for clinical use, and AD diagnosis is based on cortical amyloid ligand uptake. Amyloid ligands tend to have nonspecific uptake in the white matter, and thus the clinician should focus on the poor distinction of the cortical–subcortical junction as pathology enters the cortex. (**B**) Tau PET using AV1451 tracer. This image is provided by courtesy of Dr. Gil Rabinovici and Viktoriya Bourakova.
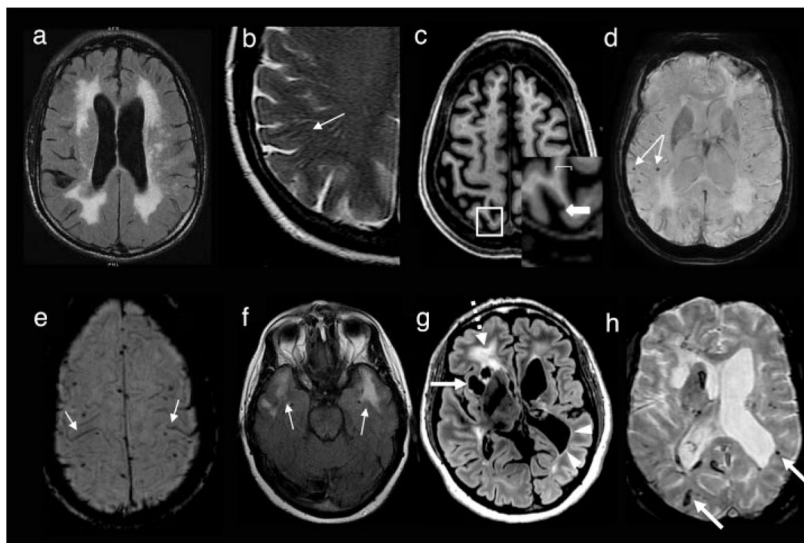
Fig. 3. Neuroimaging in vascular dementia

(**A**) Subcortical and periventricular white matter hyperintensities (WMH) in sporadic small vessel disease (SVD) on T2/FLAIR (fluid-attenuated inversion recovery). (**B**) Enlarged Virchow–Robin spaces (eVRS) on T2 sequence. (**C**) Cortical microinfarct shown as a hypointense T1 lesion. (**D**) Cortical microbleeds on T2* SWI sequence. (**E**) Superficial siderosis on T2* susceptibility-weighted imaging (SWI). (**F**) Anterior temporal lobe WMH in CADASIL on T2/FLAIR. (**G,H**) Axial MRI in a 46-year-old woman with *COL4A1* mutation and medically refractory seizures, long-standing cognitive decline and right hemiparesis since early childhood. Axial T2 FLAIR (**G**) image shows extensive white matter signal abnormality (dotted arrow), with white matter cysts (arrow), and porencephaly (arrowheads). Axial susceptibility-sensitive image at the same level (**H**) reveals multiple remote hemorrhages of varying size throughout the brain (arrows as examples). Part (c) used with permission from Hilal S, Sikking E, Shaik MA, et al. Cortical cerebral microinfarcts on 3T MRI: a novel marker of cerebrovascular disease. Neurology 2016;87(15):1583–1590. https://doi.org/10.1212/WNL.0000000000003110.
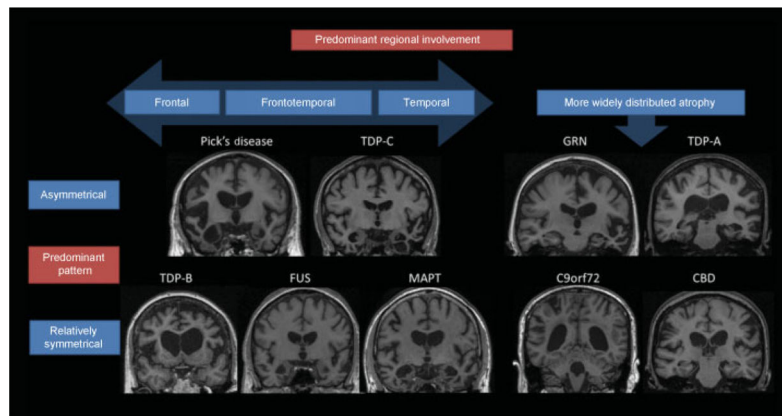
Fig. 4. Neuroimaging in pathologically confirmed frontotemporal dementia (FTD) patients
T1 MRI images in genetic and pathological forms of FTD, highlighting pathological propensities toward symmetry and regional predilections. Figure used with permission from: Gordon E, Rohrer JD, Fox NC. Advances in neuroimaging in frontotemporal dementia. J Neurochem 2016;138:193–210. https://doi.org/10.1111/jnc.13656.
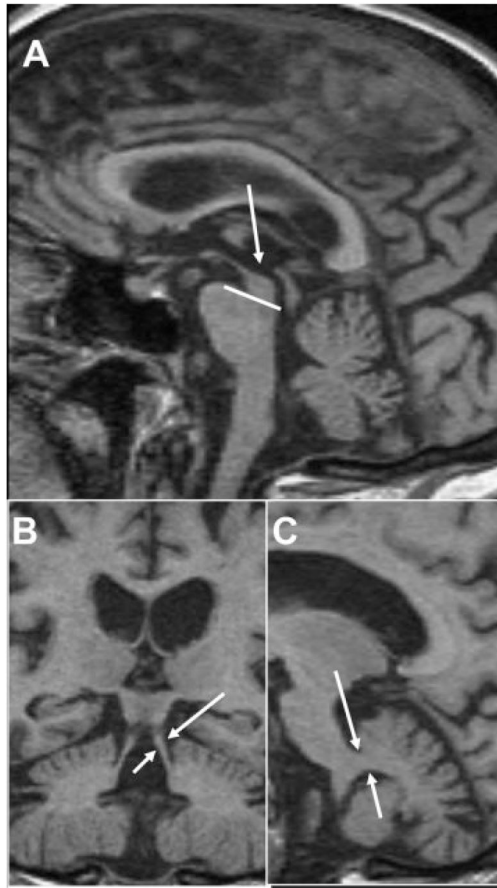
Fig. 5. Neuroimaging in progressive supranuclear palsy syndrome (PSPS)
(**A,B**) Sagittal and (C) coronal T1-weighted images from a 61-year-old man with PSPS
(MMSE 27) and autopsy-proven FTLD-PSP pathology. (**A**) Reduced midbrain area (arrow)
compared with the pons. Thinned superior cerebellar peduncles on coronal section (**B**;
arrows) are observed compared with the middle cerebral peduncles (**C**; arrows). Adapted
with permission from Vitali P, Migliaccio R, Agosta F, Rosen H, Geschwind M.
Neuroimaging in dementia. Semin Neurol 2008;28(4):467–483.
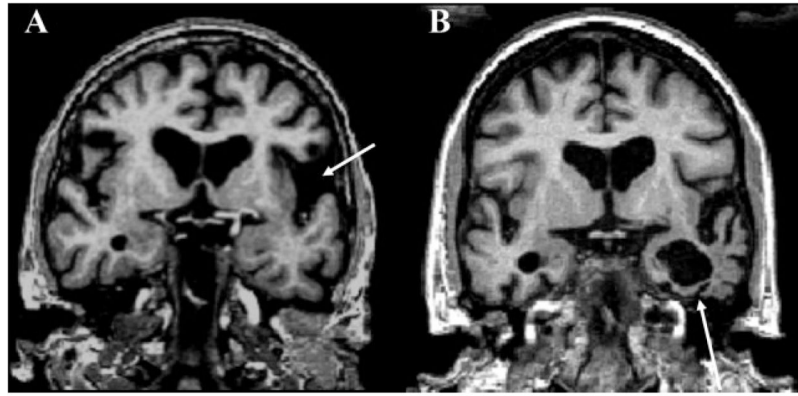
Fig. 6. Coronal T1-weighted MRI in patients with primary progressive aphasias (PPA)
(**A**) nfvPPA in a 66-year-old woman, MMSE: 28. Left predominant atrophy of the operculum is evident (arrow). (**B**) svPPA in a 66-year-old man with MMSE: 26. Atrophy is most prominent in the left perisylvian region, including the medial temporal lobes (arrow). Adapted with permission from Vitali P, Migliaccio R, Agosta F, Rosen H, Geschwind M. Neuroimaging in dementia. Semin Neurol 2008;28(4):467–483.
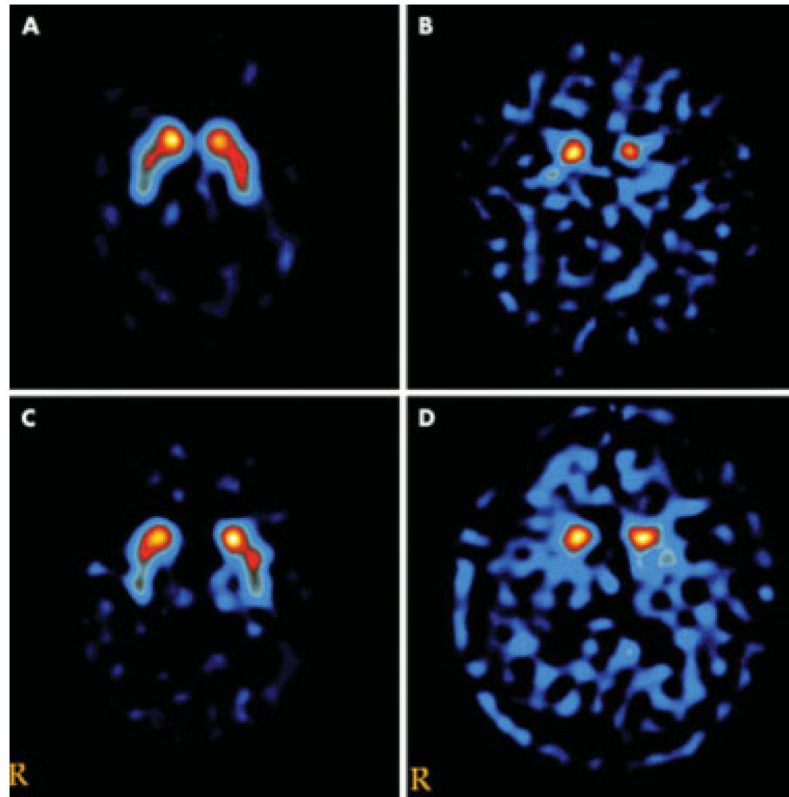
Fig. 7.
DaTSCAN (FP-CIT) in a healthy control (**A**) and patients with Parkinson's disease (**B**), Alzheimer's disease (**C**), and dementia with Lewy bodies (**D**). Used with permission from Walker Z, Costa DC, Walker RW H, et al. Differentiation of dementia with Lewy bodies from Alzheimer's disease using a dopaminergic presynaptic ligand. J Neurol Neurosurg Psychiatry 2002;73(2):134–140.
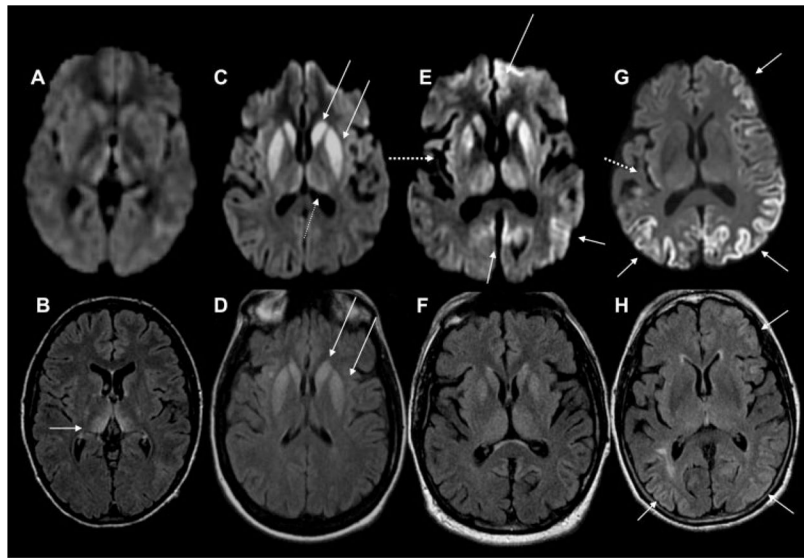
Fig. 8. Magnetic resonance imaging(MRI) findings in pathologically proven Jakob–Creutzfeldt disease (JCD)

Note that in sporadic JCD the abnormalities are usually more evident on diffusion-weighted imaging (DWI) (**C,E,G**) than on fluid-attenuated inversion recovery (FLAIR) images (**D,F,H**). Orientation is radiologic, with right side of image being left side of the brain. (**A,B**) A 21-year-old woman with probable variant JCD. MRI shows the "double hockey stick sign": bilateral thalamic hyperintensity in the mesial pars (mainly dorsomedian nucleus) and posterior pars (pulvinar) of the thalamus. Also note the "pulvinar sign," with the right posterior thalamus (pulvinar) being more hyperintense than the anterior putamen on the FLAIR image (**B**). (**C,D**) A 52-year-old woman with MRI showing strong hyperintensity in bilateral striatum (solid arrows, both caudate and putamen) and slight hyperintensity in mesial and posterior thalamus (dotted arrow). (**E,F**) A 68-year-old man with MRI showing hyperintensity in bilateral striatum (note anteroposterior gradient in the putamen, which is commonly seen in JCD), thalamus, right insula (dotted arrow), anterior and posterior cingulate gyrus (arrow, L > R), and left temporal-parietal-occipital junction (arrow). (**G,H**) A 76-year-old woman with MRI showing diffuse hyperintense signal mainly in bilateral parietal and occipital cortex, right posterior insula (dashed arrow), and left inferior frontal cortex (arrow), but no significant subcortical abnormalities. Reprinted with permission from Vitali P, Migliaccio R, Agosta F, Rosen H, Geschwind M. Neuroimaging in dementia. Semin Neurol 2008;28(4):467–483.
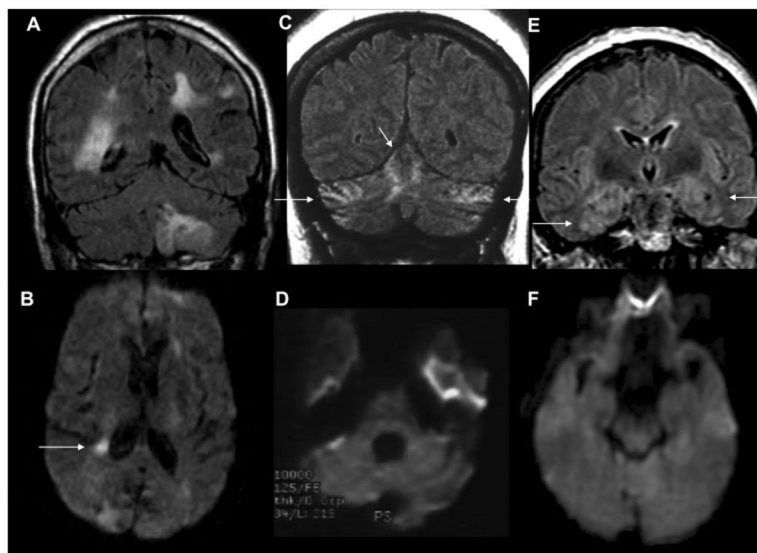
Fig. 9. Nonprion rapidly progressive dementia and ataxia syndromes

Note that in these cases, the abnormalities are seen better on the FLAIR (**A,C,E**) that the DWI (**B,C,F**) images. Orientation is radiologic, with right side of image being the left side of the brain. (**A,B**) A 66-year-old man with intravascular lymphoma. (**A**) FLAIR multifocal abnormalities involving cerebral and cerebellar gray and white matter in a vascular distribution. These lesions, also involving the right hippocampus, showed patchy enhancement after contrast administration (not shown). (**B**) DWI shows a right periventricular focal region with diffusion restriction; DWI hyperintensity is common in lymphomas. (**C,D**) A 65-year-old woman with anti-Yo paraneoplastic cerebellitis. Magnetic resonance imaging (MRI) shows mild diffuse hyperintensity of the cerebellar, compared with the cerebral, cortex with slight atrophy of the lateral folia. Note (**C**) the strong hyperintense FLAIR signal in superior, medial cerebellum (arrows), and (**D**) no major hyperintensity in the axial DWI scan. (**E,F**) A 60-year-old woman with paraneoplastic limbic encephalitis and FLAIR MRI showing hyperintensity of bilateral insula, medial (arrows) and inferior temporal cortex, hippocampus, amygdala (**E**) on FLAIR and only subtle hyperintensity (**F**) on DWI. FLAIR, fluid-attenuated inversion recovery; DWI, diffusion-weighted imaging; MRI, magnetic resonance imaging. Reprinted with permission from Vitali P, Migliaccio R, Agosta F, Rosen H, Geschwind M. Neuroimaging in dementia. Semin Neurol 2008;28(4):467–483.
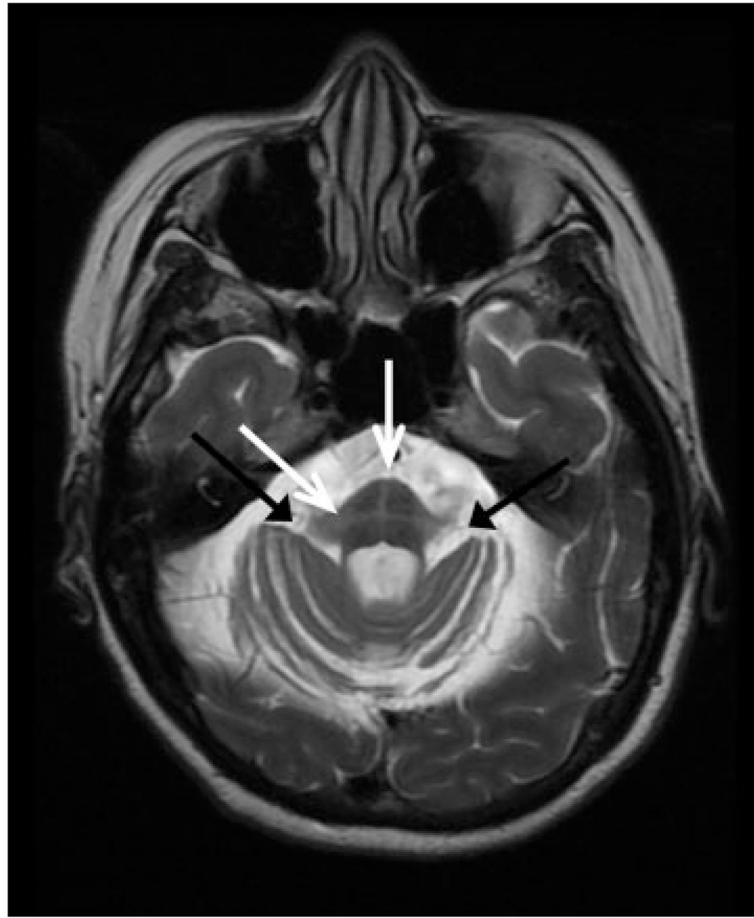
Fig. 10.
T2-weighted axial MRI of the pontine-middle cerebellar peduncle (MCP) junction in a
patient with MSA-C. Black arrows point to MCP hyperintensity. White arrows point to the
hot cross bun sign in the pons. Bilateral cerebellar hemisphere atrophy is also present.

Table 1

UCSF 2017 Proposal of MRI Criteria for JCD Diagnosis

Diagnosis	UCSF 2017 Modified JCD MRI criteria[a]
MRI definitely JCD	DWI[b] > FLAIR cortical ribboning[c] hyperintensity in:
	1. Classic pathognomonic: cingulate,[d] striatum, and > 1 neocortical gyrus (often precuneus, angular, superior parietal, superior frontal, middle frontal, or lateral temporal gyrus)
	a. Supportive for subcortical[e] involvement:
	i. Striatum with decreasing anterior–posterior gradient
	ii. Corresponding ADC hypointensity
	b. Supportive for cortical involvement:
	i. Asymmetric involvement of midline neocortex or cingulate[d]
	ii. Sparing of precentral gyrus[f]
	iii. Corresponding ADC cortical ribboning hypointensity
	2. Cortex only (> 3 gyri); see supportive for cortex (above)
MRI probably JCD	1. Unilateral striatum or cortex (3 gyri); see supportive for subcortical and cortex (above)
	2. Bilateral striatum (see supportive for subcortical) or posteromedial thalamus; see supportive for subcortical (above)
	3. DWI > FLAIR hyperintensities only in limbic areas, with corresponding ADC hypointensity[g]
MRI probably not JCD	1. Only FLAIR/DWI abnormalities only in limbic areas, where hyperintensity can be normal (e.g., insula, anterior cingulate, and hippocampi), and ADC map does not show corresponding restricted diffusion (hypointensity)
	2. DWI hyperintensities due to artifact (signal distortion); see other MRI issues (below)
	3. FLAIR > DWI hyperintensities[h]; see other MRI issues (below)
MRI definitely not JCD	1. Normal
	2. Abnormalities not consistent with JCD
Other MRI issues	In prolonged courses of sJCD (~ >1 year), brain MRI might show significant atrophy with loss of DWI hyperintensity, particularly in areas previously with restricted diffusion.
	To help distinguish abnormality from artifact, obtain b2000 diffusion sequences in multiple directions (e.g., axial and coronal).

Abbreviations: ADC, apparent diffusion coefficient; DWI, diffusion-weighted imaging; FLAIR, fluid-attenuated inversion recovery; JCD, Jakob–Creutzfeldt disease; MRI, magnetic resonance imaging.

[a] Modified from Vitali et al 2011.[215]

[b] Recommended minimum standard diffusion sequence parameters to best identify cortical ribboning: axial and coronal DWI/ADC b = 1000 second cm2 or b = 2000 second cm2, depending on scanner field strength and capabilities to achieve satisfactory image quality. At 3T, b = 2000 may be preferred due to higher contrast to background for abnormal gray matter diffusion.

[c] Involvement of cortical gray matter with sparing of underlying or adjacent white matter.

[d] Mid and posterior cingulate preferred over anterior due to anterior air-brain artifact especially on axial acquisition (anterior acceptable if coronal acquisition). Can be symmetric, but if so prefer ADC hypointensity correlate.

[e] Subcortical = deep nuclei, in decreasing order of frequency caudate, putamen, thalamus (posteriomedial or diffuse), globus pallidus (rare). ADC often shows corresponding and earlier involvement than DWI.

[f] If precentral gyrus is preferentially involved consider nonprion diagnoses (e.g., seizures and Wernicke's).

[g]DWI > FLAIR with reduced ADC in limbic or other cortical regions also can occur in HSV encephalitis[360,361] and seizures[362,363] depending on clinical picture, these should be ruled out.

[h]Consider T2-shine through.[364]